Ubiquitination-mediated Golgi-to-endosome sorting determines the poison-antidote duality of *wtf* meiotic drivers

Jin-Xin Zheng,[1,2] Tong-Yang Du,[2,3] Guang-Can Shao,[2] Zhu-Hui Ma,[2] Zhao-Di Jiang,[2] Wen Hu,[2] Fang Suo,[2] Wanzhong He,[2] Meng-Qiu Dong,[2,4] and Li-Lin Du[1,2,4,*]

[1]Graduate School of Peking Union Medical College, Beijing 100730, China

[2]National Institute of Biological Sciences, Beijing 102206, China.

[3]College of Life Sciences, Beijing Normal University, Beijing 100875, China

[4]Tsinghua Institute of Multidisciplinary Biomedical Research, Tsinghua University, Beijing 102206, China.

*Correspondence: dulilin@nibs.ac.cn

Abstract

Killer meiotic drivers (KMDs) skew allele transmission in their favor by killing meiotic progeny not inheriting the driver allele. Despite their widespread presence in eukaryotes, the molecular mechanisms behind their selfish behavior are poorly understood. Here we investigate how the poison and antidote products of a fission yeast *wtf*-family KMD gene can act antagonistically. Both the poison and the antidote are multi-transmembrane proteins, differing only in their N-terminal cytosolic tails. We find that the antidote employs N-terminal PY motifs to bind Rsp5/NEDD4 family ubiquitin ligases, which ubiquitinate the antidote. Mutating PY motifs or attaching a deubiquitinating enzyme transforms the antidote into a toxic protein. Ubiquitination promotes the transport of the antidote from the trans-Golgi network to the endosome, thereby neutralizing its toxicity and that of the bound poison. We propose that post-translational modification-mediated protein localization and/or activity changes may be a common mechanism governing the antagonistic duality of single-gene KMDs.

Keywords: killer meiotic driver, *wtf* family genes, ubiquitination, post-translational modification, *Schizosaccharomyces pombe*

Introduction

The killer meiotic drivers (KMDs), which have been found in animals, fungi, and plants, are selfish genetic elements that subvert Mendel's law of segregation by disabling meiotic progeny lacking the driver element.[1] A commonly employed mode of action of KMDs is the poison-antidote mechanism.[1] The poison-antidote KMDs express two protein products, a poison and an antidote. The poison exerts a killing activity towards all meiotic progeny and the antidote confers a protection against the poison in progeny carrying the driver allele. Interestingly, the poison and the antidote can be encoded by the same gene. Single-gene KMDs known or proposed to employ the poison-antidote mechanism include *wtf* genes of fission yeasts,[2-8] the *Spk-1* gene of *Neurospora*,[9] and the *Spok* family genes found in *Podospora* and other filamentous fungi.[10-14] How a single-gene KMD can produce proteins with antagonistic activities has been a perplexing mystery.

wtf (for with Tf LTRs) genes, which encode multi-transmembrane proteins, constitute the largest gene family in the fission yeast *Schizosaccharomyces pombe*.[7,8,15] Some of the *S. pombe wtf* genes are drivers that can express both a poison and an antidote through alternative transcription initiation, whereas others express only an antidote.[4,7,8] The poison and the antidote expressed by a *wtf* driver gene have identical transmembrane domains, differing only in their N-terminal tails, where the antidote features an extension at its N-terminus. Presumably, this antidote-specific region plays a key role in determining the distinction between the poison and the antidote. However, no activities have been assigned to the antidote-specific region.

Here, we show that the antidote-specific region is a binding platform for ubiquitin ligases and mediates the ubiquitination of the antidote. Ubiquitination directs the transport of the antidote from the trans-Golgi network (TGN) to the endosome, preventing the antidote from causing toxicity and allowing it to detoxify the poison

bound to it. This ubiquitination-mediated toxicity neutralization mechanism is conserved among *wtf* genes, including *S. pombe wtf* genes encoding only antidotes and *wtf* genes present in other fission yeast species that diverged from *S. pombe* about 100 million years ago. Our findings provide new insights into the molecular mechanisms underlying the actions of KMDs.

Results

The poison and antidote products of *cw9* are active in vegetative cells

We used the *S. pombe wtf* gene *cw9*, which is an active KMD from the natural isolate CBS5557,[8] as a model to study the molecular mechanism underlying the distinction between the poison and the antidote. We named its poison Cw9ki (the killing isoform) and its antidote Cw9pi (the protecting isoform). Cw9pi is 52 amino acids longer than Cw9ki at the N terminus (Figure 1A). Transcripts encoding Cw9pi and Cw9ki are initiated from upstream of coding exon 1 and within intron 1, respectively. As shown before,[8] the removal of the sequence upstream of exon 1 resulted in a form of *cw9* that indiscriminately kills spore progeny of a hemizygous cross between a strain carrying this form of *cw9* and a strain without *cw9*, presumably because only Cw9ki but not Cw9pi can be expressed (Figure 1B). On the other hand, a Cw9pi-only form created through deleting intron 1 was able to protect progeny from the killing effect of Cw9ki expressed from a different locus (Figure 1B). Thus, Cw9ki and Cw9pi can act as poison and antidote respectively when they are not expressed from the same locus.

It has been shown that both the poison and antidote products of the *Sk wtf4* gene from the *S. pombe var. kambucha* strain are active in vegetative cells.[5] To test whether the toxicity of Cw9ki can manifest in vegetative *S. pombe* cells, we placed its coding sequence under the control of thiamine-repressible promoters (*Pnmt1*, *P41nmt1*, or *P81nmt1*, from the strongest to the weakest) (Figure 1C).[16]

88 We found that Cw9ki expressed from the *P81nmt1* or *P41nmt1* promoter
89 prevented the growth of vegetative cells under the induction condition (minus
90 thiamine) (Figure 1C). We failed to obtain strains expressing Cw9ki from the
91 strongest *Pnmt1* promoter, probably due to toxicity caused by a higher level of
92 basal expression. Cw9ki expressed from the anhydrotetracycline (ahTet)-inducible
93 promoter *PtetO7* also showed strong toxicity to vegetative cells under the induction
94 condition (Figure S1A).[17] Thus, Cw9ki is a poison that can kill not only *S. pombe*
95 spores, but also *S. pombe* vegetative cells.

96 When examining cells using differential interference contrast (DIC) microscopy,
97 we found that Cw9ki induction in vegetative cells resulted in the appearance of
98 large crater-like structures (Figures 1D and S1B). We suspected that these
99 structures may correspond to enlarged vacuoles. Indeed, Zhf1, a vacuole
100 membrane marker, localized at the boundaries of the structures, and Cpy1, a
101 vacuole lumen marker, localized in the interior of the structures (Figure 1D).
102 Enlarged vacuoles can also be observed by electron microscopy analysis (Figure
103 S1C). The reason behind this phenotype is unclear, but it serves as a convenient
104 readout of the toxicity of Cw9ki in vegetative *S. pombe* cells.

105 To test whether Cw9pi can act in vegetative cells, we placed its coding sequence
106 (without intron 1) under the control of thiamine-repressible promoters (Figure 1E).
107 Inducing the expression of Cw9pi had no effect on vegetative cell growth, even
108 when using the strongest *Pnmt1* promoter. When we co-expressed Cw9pi and
109 Cw9ki, the toxicity of Cw9ki expressed from the *P41nmt1* promoter was completely
110 abrogated by Cw9pi expressed from either the *P41nmt1* promoter or the *Pnmt1*
111 promoter and strongly but incompletely mitigated by Cw9pi expressed from the
112 weakest *P81nmt1* promoter (Figure 1E), indicating that the protecting activity
113 conferred by Cw9pi is dose-dependent. When Cw9ki was expressed from the
114 *P81nmt1* promoter, co-expressing Cw9pi from even the *P81nmt1* promoter can

115 abolish the toxicity (Figure S1D).

116 We also tested whether Cw9ki and Cw9pi are active in the vegetative cells of
117 the budding yeast *Saccharomyces cerevisiae*. Similar to the observations made
118 on the products of *Sk wtf4*,[5] we found that Cw9ki was toxic to vegetative budding
119 yeast cells, and Cw9pi can neutralize the toxicity of Cw9ki in a dose-dependent
120 manner (Figures S1E and S1F). Together, our results indicate that the activities of
121 Cw9ki and Cw9pi are neither specific to spores nor limited to *S. pombe*.

122

123 **The antidote-specific region binds Rsp5/NEDD4 family ubiquitin ligases**

124 Cw9pi is predicted to be a multi-transmembrane protein with both its N terminus
125 and C terminus in the cytosol (Figure S1G).[8] Its most N-terminal 52 amino acids,
126 which are absent in Cw9ki, are part of the N-terminal cytosolic tail, which is
127 predicted to be 105 amino acids long (Figure 2A). How does the presence or
128 absence of this antidote-specific region, Cw9pi(1-52), determine whether the
129 protein is an antidote or a poison? As Cw9pi is essentially a combination of
130 Cw9pi(1-52) and Cw9ki, we first addressed the question of how the presence of
131 Cw9pi(1-52) in the same polypeptide with Cw9ki prevents the manifestation of the
132 toxicity of Cw9ki. We hypothesized that Cw9pi(1-52) may possess an activity that
133 can neutralize the toxicity of Cw9ki as long as it is physically associated with Cw9ki.
134 To test this idea, we artificially tethered Cw9pi(1-52) to Cw9ki using the
135 noncovalent interaction between GFP and GBP (GFP binding protein).[18,19] We co-
136 expressed a GFP-tagged form of Cw9ki, which is toxic to *S. pombe* vegetative cells
137 (Figure 2B), with Cw9pi(1-52) or Cw9pi(1-52) fused with GBP. Cw9pi(1-52) did not
138 obviously ameliorate the toxicity of GFP-Cw9ki, whereas Cw9pi(1-52)-GBP
139 abolished the toxicity of GFP-Cw9ki (Figure 2B), supporting the idea that Cw9pi(1-
140 52) possesses a toxicity-neutralizing activity that can detoxify associated Cw9ki.

141 To explore the molecular mechanism underlying the toxicity-neutralizing activity

142 of Cw9pi(1-52), we searched for physical interactors of Cw9pi(1-52) using affinity
143 purification coupled with mass spectrometry (AP-MS). One hit of the AP-MS
144 analysis is Pub1 (Figure 2C), an Rsp5/NEDD4 family ubiquitin ligase.[20] In *S.*
145 *pombe*, there are three Rsp5/NEDD4 family ubiquitin ligases, Pub1, Pub2, and
146 Pub3.[21] Pub1 and Pub3 are more similar to each other than to Pub2 and are
147 redundantly essential for cell growth.[21] Pub1 has the highest expression level
148 among the three.[22,23] We used the GST pulldown assay to examine whether
149 Cw9pi(1-52) interacts with these three ubiquitin ligases and found that both Pub1
150 and Pub3 exhibited robust interactions with Cw9pi(1-52), whereas Pub2 showed
151 a much weaker interaction with Cw9pi(1-52) (Figure 2D).
152 The ability of Cw9pi(1-52) to interact with Rsp5/NEDD4 family ubiquitin ligases
153 led us to hypothesize that Cw9pi(1-52) may neutralize the toxicity of associated
154 Cw9ki through recruiting ubiquitin ligases. This hypothesis predicts that the toxicity
155 of Cw9ki may be inhibited if a ubiquitin ligase is artificially tethered to it. To test this
156 idea, we employed the GFP–GBP interaction again. Indeed, tethering Pub1 to
157 Cw9ki abolished the toxicity of Cw9ki (Figure 2E). As a control, tethering Pub1-
158 C735S, a catalytically dead mutant of Pub1,[24] to Cw9ki did not affect the toxicity,
159 indicating that the ubiquitin ligase activity is required for neutralizing the toxicity.
160 Artificially tethering Pub3 to Cw9ki can also abolish the toxicity, whereas tethering
161 Pub2 only partially neutralized the toxicity (Figure 2F). These results suggest that
162 the antidote-specific region of Cw9pi acts as a binding platform for Rsp5/NEDD4
163 family ubiquitin ligases, especially Pub1 and Pub3, and these ubiquitin ligases,
164 when recruited near Cw9ki, can neutralize the toxicity of Cw9ki through promoting
165 ubiquitination.
166
167 **PY motifs in the N-terminal tail of Cw9pi are responsible for binding ubiquitin**
168 **ligases and preventing Cw9pi from becoming toxic**

169 The substrate proteins of Rsp5/NEDD4 family ubiquitin ligases often contain one
170 or multiple [L/P]PxY sequences (PY motifs), which are binding sites of the WW
171 domains in the Rsp5/NEDD4 family ubiquitin ligases.[25-27] There are three PY motifs
172 in Cw9pi, at positions 30-33, 41-44, and 69-72, respectively (Figure 3A). We
173 named them PY1, PY2, and PY3. PY1 and PY2 are located within the antidote-
174 specific region. In a sequence alignment of the N-terminal cytosolic tails of the
175 antidote products of two active *wtf* driver genes from CBS5557 (*cw9* and *cw27*)
176 and 16 non-pseudo *wtf* genes in the *S. pombe* reference genome, PY1 and PY2
177 are conserved in the products of all but the four most divergent *wtf* genes (*wtf7*,
178 *wtf11*, *wtf14*, and *wtf15*), which do not have KMD activities,[4] whereas PY3 is only
179 present in the products of four genes, *cw9*, *cw27*, *wtf19*, and *wtf23* (Figure 3A).
180 The absence of PY3 in the product of the known active driver gene *wtf13* suggests
181 that PY3 is not essential for the selfish actions.[6]

182 To examine whether the PY motifs in the N-terminal cytosolic tail of Cw9pi
183 mediate interactions with Rsp5/NEDD4 family ubiquitin ligases, we performed GST
184 pulldown analysis using *E. coli*-expressed Cw9pi N-terminal fragments fused with
185 GST and *E. coli*-expressed Pub1 lacking the N-terminal C2 domain but containing
186 all three WW domains (Pub1-ΔC2) (Figure 3B). It is known that mutating the strictly
187 conserved tyrosine residue in a PY motif to alanine disrupts the ability of the PY
188 motif to bind WW domains.[28,29] Thus, we introduced into the PY motifs of Cw9pi
189 such tyrosine-to-alanine mutations (denoted by asterisks). Mutating the three PY
190 motifs individually (PY1*, PY2*, or PY3*) did not obviously affect the ability of the
191 N-terminal cytosolic tail of Cw9pi, Cw9pi(1-104) (abbreviated as N in Figure 3B),
192 to bind Pub1-ΔC2. When two out of the three PY motifs were mutated
193 simultaneously, the PY1*PY2* and PY2*PY3* combinations, but not the PY1*PY3*
194 combination, resulted in dramatically reduced but still detectable interactions.
195 Disrupting all three PY motifs (3PY*) weakened the interaction to an undetectable

196 level. Consistently, Cw9pi(24-52), a 29-amino-acid fragment containing both PY1
197 and PY2, interacted with Pub1-ΔC2 as strongly as Cw9pi(1-104). Cw9pi(53-104),
198 which contains only PY3, interacted weakly with Pub1-ΔC2, whereas Cw9pi(1-23)
199 that lacks any PY motifs did not interact with Pub1-ΔC2 (Figure 3B). Similar results
200 were obtained when using Pub3 as prey to perform GST pulldown assay (Figure
201 S2A). Together, these results indicate that the three PY motifs of Cw9pi act
202 redundantly to promote interactions with Pub1 and Pub3. PY2 is sufficient to
203 mediate a strong interaction by itself, whereas PY1 and PY3 individually are much
204 weaker binding motifs but together can mediate a robust interaction.

205 To examine the in vivo roles of the PY motifs, PY-mutated forms of Cw9pi were
206 expressed in vegetative *S. pombe* cells using the inducible *P81nmt1* promoter.
207 Mutations that did not substantially affect Pub1/Pub3 binding in the GST pulldown
208 analysis, including PY1*, PY2*, PY3*, and PY1*PY3*, did not alter the non-toxic
209 nature of Cw9pi (Figures 3C and S2B). In contrast, mutations that markedly
210 weakened ubiquitin ligase binding in the pulldown assay, including PY1*PY2*,
211 PY2*PY3*, and 3PY*, rendered Cw9pi strongly toxic to vegetative cells (Figure 3C).
212 Thus, PY motif-mediated binding to Rsp5/NEDD4 family ubiquitin ligases keeps
213 Cw9pi in a non-toxic state.

214 We found that the 3PY* mutation can also convert Cw9pi from non-toxic to toxic
215 in vegetative *S. cerevisiae* cells (Figure S2C), indicating that PY motifs in Cw9pi
216 can mediate toxicity neutralization in *S. cerevisiae*, probably because PY motif
217 binding is a conserved feature of Rsp5/NEDD4 family ubiquitin ligases, which are
218 ubiquitously present in fungi and animals.[30]

219 To examine whether PY motifs are also important for preventing Cw9pi from
220 becoming toxic during sexual reproduction, we placed Cw9pi-3PY* under the
221 control of the native upstream sequence. This form, referred to as *cw9pi-3PY**, can
222 only be introduced into a strain that also contains a wild-type form of *cw9pi*,

223 presumably because of the toxicity of Cw9pi-3PY* to vegetative cells. When the
224 strain containing both *cw9pi-3PY** and *cw9pi* was crossed to a strain without any
225 forms of *cw9*, spores containing *cw9pi-3PY** but not *cw9pi* were all inviable,
226 whereas other spores were mostly viable (Figure 3D). Thus, *cw9pi-3PY** behaved
227 as a suicidal gene during sexual reproduction, indicating that PY motif-mediated
228 ubiquitin ligase binding is required to prevent the antidote from becoming a poison
229 in the native context of KMD actions.

230 PY3 is located downstream of the antidote-specific region and thus is present in
231 Cw9ki. The pulldown analyses showed that PY3 can support a weak binding with
232 Pub1 and Pub3 (Figures 3B and S2A). To determine whether the presence of PY3
233 weakens the toxicity of Cw9ki, we expressed Cw9ki in vegetative cells using an
234 attenuated version of the *P81nmt1* promoter (*P81nmt1a*) so that cell growth was
235 inhibited but not completely prevented. We found that mutating PY3 of Cw9ki did
236 not alter the extent of growth inhibition (Figure S2D), indicating that PY3 does not
237 influence the toxicity of Cw9ki, perhaps because PY3-mediated ubiquitin ligase
238 binding is too weak to reach a threshold needed to exert a neutralizing effect on
239 the toxicity.

240 To further ascertain the toxicity-neutralizing role of PY motifs, we tested whether
241 simply adding a strong exogenous PY motif to Cw9ki is sufficient to neutralize its
242 toxicity. We fused to the N-terminus of Cw9ki a PY-motif-containing artificial
243 peptide (artPY, MPSTP<u>PPPY</u>SRGT), which is known to promote strong in vitro
244 ubiquitination by the Rsp5 ubiquitin ligase.[31] This fusion abolished the toxicity of
245 Cw9ki (Figure 3E). As a control, fusing a PY-mutated peptide (artPY*,
246 MPSTP<u>PPPA</u>SRGT) to Cw9ki did not affect the toxicity. When artPY-Cw9ki and
247 Cw9ki were co-expressed, artPY-Cw9ki behaved like an antidote and neutralized
248 the toxicity of Cw9ki (Figure 3E). Thus, the antidote-specific region of Cw9pi can
249 be substituted by an exogenous PY motif, indicating that the main function of the

250 antidote-specific region is binding Rsp5/NEDD4 family ubiquitin ligases through
251 PY motifs.
252
253 **Ubiquitination sites in the N-terminal cytosolic tail of Cw9pi are necessary**
254 **for preventing Cw9pi from becoming toxic**
255 Because the N-terminal cytosolic tail of Cw9pi interacts with Rsp5/NEDD4 family
256 ubiquitin ligases, we tested whether this region of Cw9pi harbors ubiquitination
257 sites that can be modified by Rsp5/NEDD4 family ubiquitin ligases. We performed
258 in vitro ubiquitination reactions using recombinant Cw9pi(1-104) as the substrate
259 and recombinant Pub1-ΔC2 as the E3 (Figure 4A). Pub1-ΔC2 lacks the N-terminal
260 membrane-binding C2 domain but contains the catalytic domain and all three WW
261 domains. Upon SDS-PAGE separation of the reaction mixes, we observed that the
262 unmodified form of Cw9pi(1-104) decreased and higher molecular weight forms of
263 Cw9pi(1-104) appeared when and only when ubiquitin, E1, E2, and E3 were all
264 present, indicative of ubiquitination of Cw9pi(1-104). The extent of ubiquitination
265 correlated with the amount of E3. Thus, Cw9pi(1-104) is a ubiquitination substrate
266 of Pub1.
267 To test whether PY motifs are important for the ubiquitination of Cw9pi(1-104)
268 by Pub1, we performed ubiquitination reactions on PY-mutated Cw9pi(1-104)
269 proteins (Figure 4B). Mutating the three PY motifs individually caused mild
270 reduction of ubiquitination, with PY2* showing the strongest effect. Among the
271 double PY mutations, PY1*PY2* and PY2*PY3* but not PY1*PY3* mutations
272 caused substantially more severe reduction of ubiquitination than PY2*. 3PY*
273 mutations reduced the ubiquitination to an undetectable level. These results
274 parallel the binding assay results shown earlier, and indicate that PY motifs are
275 needed for the ubiquitination of Cw9pi(1-104) by Pub1.
276 To obtain evidence on the in vivo role of Cw9pi ubiquitination, we tested whether

277 artificially preventing the ubiquitination of Cw9pi can render it toxic. We tethered
278 UL36, a deubiquitinating enzyme (DUB), to Cw9pi using the GFP–GBP
279 interaction.[32-35] Cw9pi fused at the N terminus with mECitrine, a variant of GFP,
280 was expressed from the thiamine-repressible *P81nmt1* promoter and DUB fused
281 with GBP was expressed from the ahTet-inducible *PtetO7* promoter. The co-
282 expression of GBP-DUB, but not the catalytically inactive GBP-DUB*, with
283 mECitrine-Cw9pi caused toxicity to vegetative *S. pombe* cells (Figure 4C),
284 indicating that ubiquitination of Cw9pi is essential for preventing it from becoming
285 toxic.

286 There are a total of 16 lysines in the cytosolic tails and loops of Cw9pi (Figure
287 4D). We predicted that mutating all these lysines should prevent Cw9pi from being
288 ubiquitinated and render Cw9pi toxic. Indeed, when all 16 lysines were mutated to
289 arginines, the resulting mutant, Cw9pi-16R, was toxic to vegetative cells (Figure
290 4E). Next, to define a minimal set of ubiquitination sites important for toxicity
291 neutralization, we mutated only the lysines in the N-terminal cytosolic tail. There
292 are seven lysines in this region (Figures 4D and 4F). Mutating the five lysines in
293 the antidote-specific region (Cw9pi-5R) or mutating the two lysines in the
294 remaining portion of the N-terminal cytosolic tail (Cw9pi-2R) had no effect,
295 whereas mutating all seven lysines (Cw9pi-7R) rendered Cw9pi toxic (Figure 4F).
296 Reverting any one of the seven mutations back to lysine abolished the toxicity of
297 Cw9pi-7R (Figure 4G), suggesting that these seven lysines can all be ubiquitinated
298 and the ubiquitination of these lysines is redundantly required for toxicity
299 neutralization. Consistently, using mass spectrometry analysis, we found that all
300 seven lysines in the N-terminal cytosolic tail can be ubiquitinated in vitro by Pub1
301 or Pub3 (Figures 4H and S2E). Together, these results indicate that PY motif-
302 dependent ubiquitination of the N-terminal cytosolic tail of Cw9pi is necessary for
303 preventing Cw9pi from becoming toxic.

304

305 **The vacuolar targeting of Cw9pi is mediated by the ESCRT machinery**

306 It has been reported that the antidote and the poison products of the *Sk wtf4* gene
307 from the *S. pombe var. kambucha* strain exhibited distinct subcellular localization
308 patterns, with the antidote protein localizing to vacuoles and the poison protein
309 forming cytoplasmic puncta.[5,7] To examine the localization of the protein products
310 of *cw9*, we performed microscopy analysis on Cw9ki and Cw9pi tagged with
311 fluorescent proteins. Cw9ki was tagged by inserting a fluorescent protein at an
312 internal position of the N-terminal cytosolic tail (between S96 and G97, amino acid
313 numbering based on the sequence of Cw9pi), because this way of tagging
314 maintained the spore killing activity of Cw9ki better than C-terminal tagging or N-
315 terminal tagging (Figure S3A). We refer to Cw9ki tagged internally with GFP as
316 GFP^{int}-Cw9ki. Cw9pi was tagged at the N terminus, as N-terminal tagging did not
317 obviously affect the antidote activity of Cw9pi (Figure S3B). Similar to the
318 observations made on the protein products of *Sk wtf4*,[5,7] GFP-Cw9pi showed
319 perfect co-localization with the vacuole lumen marker Cpy1-CFP in spores (Figure
320 S3C), whereas GFP^{int}-Cw9ki formed puncta not overlapping with vacuoles in
321 spores (Figure S3D).

322 In vegetative cells, Cw9ki and Cw9pi tagged with the yellow fluorescent protein
323 mECitrine and expressed from the *P81nmt1* or *P41nmt1* promoter behaved like
324 the untagged proteins in terms of the toxicity of Cw9ki and the antidote activity of
325 Cw9pi (Figure S3E). Similar to the situation in spores, in vegetative cells,
326 $mECitrine^{int}$-Cw9ki formed cytoplasmic puncta and mECitrine-Cw9pi localized to
327 the vacuole lumen (Figure 5A). mECitrine-Cw9pi localized in the vacuole lumen is
328 expected to be cleaved by vacuolar proteases to release free mECitrine, which is
329 resistant to protease digestion.[36] Indeed, immunoblotting analysis showed that
330 mECitrine-Cw9pi was processed into free mECitrine in vegetative cells in a manner

331 dependent on the two main vacuolar proteases Isp6 and Psp3 (Figure 5B).[37]

332 It has been shown that the co-expression of *Sk wtf4* antidote protein results in
333 the relocalization of *Sk wtf4* poison protein to vacuoles.[5] Similarly, we found that
334 the co-expression of mCherry-Cw9pi altered the localization of mECitrine^{int}-Cw9ki
335 in vegetative *S. pombe* cells, resulting in a perfect co-localization of mECitrine^{int}-
336 Cw9ki with mCherry-Cw9pi in the vacuole lumen (Figure 5C). This effect of Cw9pi
337 on Cw9ki is likely mediated by a physical interaction between Cw9pi and Cw9ki,
338 as mCherry-Cw9pi can be co-immunoprecipitated with mECitrine^{int}-Cw9ki (Figure
339 5D). Thus, as proposed before for *Sk wtf4*,[5] Cw9pi may exert its antidote activity
340 through binding Cw9ki and altering the localization of Cw9ki.

341 Because mutating PY motifs in the N-terminal cytosolic tail of Cw9pi can render
342 Cw9pi toxic, we hypothesized that PY-mutated forms of Cw9pi that become toxic
343 may have a localization pattern similar to that of Cw9ki. Indeed, toxic Cw9pi
344 mutants, including PY1*PY2*, PY2*PY3*, and 3PY* mutants, no longer showed
345 prominent vacuolar localization but instead mainly localized to cytoplasmic puncta,
346 whereas non-toxic PY-mutated forms of Cw9pi, including PY1*, PY2*, PY3*, and
347 PY1*PY3*, still mainly localized to the vacuole lumen (Figure 5E). Thus, the
348 targeting of Cw9pi to the vacuole lumen requires the PY motifs.

349 Ubiquitination of transmembrane proteins by Rsp5/NEDD4 family ubiquitin
350 ligases is known to be a sorting signal recognized by the endosomal sorting
351 complex required for transport (ESCRT) machinery.[38] The ESCRT machinery sorts
352 ubiquitinated transmembrane proteins into intra-endosomal vesicles, which end up
353 in the vacuole lumen upon endosome-vacuole fusion. As the PY motifs in Cw9pi
354 promote the ubiquitination of Cw9pi by Rsp5/NEDD4 family ubiquitin ligases, we
355 hypothesized that the vacuolar targeting of Cw9pi may rely on the ESCRT
356 machinery. Supporting this idea, we found that in the absence of Vps24, a
357 component of the ESCRT-III complex, Cw9pi no longer localized to the vacuole

358 lumen (Figure 5F), and instead formed cytoplasmic puncta, which tend to be larger
359 than the puncta formed by Cw9ki. These Cw9pi puncta showed substantial co-
360 localization with two endosome markers: the ESCRT-0 complex subunit Hse1 and
361 the endosomal membrane protein SPAC15A10.06 (ortholog of *S. cerevisiae* Nhx1)
362 (Figures 5F and 5G), suggesting that Cw9pi accumulates on the endosome when
363 the ESCRT machinery is defective. Thus, Cw9pi is transported to the vacuole
364 through the endosome and the ESCRT machinery is required for the endosome-
365 to-vacuole transport of Cw9pi.

366 The ubiquitination on the cargo transmembrane proteins transported by the
367 ESCRT machinery is known to be removed by DUBs when the cargo proteins are
368 sequestered into the endosome.[39] The transient nature of ubiquitination makes its
369 in vivo detection challenging. An ESCRT mutant preventing the endosomal
370 sequestration of cargo proteins, such as *vps24Δ*, causes the accumulation of
371 ubiquitinated cargo proteins and makes their detection easier.[40] Using biotin-
372 tagged ubiquitin (biotin-Ub) to enrich ubiquitinated proteins,[34,41] we detected
373 ubiquitinated Cw9pi in *vps24Δ* cells (Figure 5H). The PY1*PY3* mutation, which
374 does not prevent the vacuolar localization of Cw9pi in the wild-type background,
375 diminished but did not abolish ubiquitination in *vps24Δ* cells, whereas PY1*PY2*,
376 PY2*PY3*, and 3PY* mutations, which prevent the vacuolar localization of Cw9pi
377 in the wild-type background, decreased ubiquitination to an undetectable level in
378 *vps24Δ* cells (Figure 5H). These results support that PY motif-mediated
379 ubiquitination determines the endosome-to-vacuole transport of Cw9pi.

380

381 **Trafficking of Cw9pi and Cw9ki from the TGN to the endosome prevents their**
382 **toxicity**

383 Although deleting *vps24* prevented the vacuolar targeting of Cw9pi, Cw9pi did not
384 show toxicity in *vps24Δ* cells (Figure 5I). This is not due to a suppression effect of

385 *vps24Δ* on the manifestation of toxicity, as Cw9ki and PY-mutated forms of Cw9pi
386 showed toxicity in *vps24Δ* cells (Figure S3F). Thus, ubiquitination-dependent
387 neutralization of the toxicity of Cw9pi still occurs when Cw9pi localizes at the
388 endosome. We predicted that in this situation, Cw9pi can also act as an antidote
389 to inhibit the toxicity of Cw9ki. Indeed, mTurquoise2-Cw9pi neutralized the toxicity
390 of mECitrine^{int}-Cw9ki in *vps24Δ* cells (Figure 5J). Moreover, they co-localized with
391 the endosome marker Hse1 (Figure S3G). In contrast, Cw9ki and Cw9pi-3PY*,
392 when individually expressed, did not show obvious co-localization with Hse1 in
393 *vps24Δ* cells (Figure S3H). These results suggest that endosomal localization
394 prevents Cw9pi and Cw9ki from becoming toxic.

395 To determine which compartment Cw9ki localizes to in the absence of Cw9pi,
396 we performed co-localization analysis using a number of organelle markers
397 exhibiting punctate patterns and found that mECitrine^{int}-Cw9ki puncta partially co-
398 localized with the trans-Golgi network (TGN) marker Sec72-mCherry (Figure S3I).
399 The TGN is a dynamic organelle and typical TGN-localizing proteins only exhibit
400 partial overlap with each other.[42] We performed a time-lapse analysis and found
401 that the cytoplasmic puncta of Cw9ki exhibited dynamic behaviors and showed
402 transient co-localization with Sec72 puncta (Figure 5K). The most likely trafficking
403 route that Cw9ki takes to reach the TGN is the secretary pathway starting at the
404 endoplasmic reticulum (ER). Supporting this idea, overexpressing a dominant
405 negative Sar1-T34N mutant, which impedes ER-to-Golgi transport at the ER exit
406 step,[43] caused mECitrine^{int}-Cw9ki to show a perfect co-localization with the ER
407 marker Ost4-mCherry (Figure S3J). These results suggest that Cw9ki enters the
408 secretary pathway at the ER and is transported through the Golgi to reach the TGN.

409 We hypothesized that Cw9pi follows the same trafficking route as Cw9ki to reach
410 the TGN, where the ubiquitination sorting signal on Cw9pi directs its transport to
411 the endosome. This hypothesis predicts that ubiquitin-binding trafficking factors

412 may promote the TGN-to-endosome transport of Cw9pi. The most obvious
413 candidates for such factors are Golgi-localized gamma-ear-containing ARF-
414 binding (GGA) family trafficking adaptors that can bind ubiquitin and act in TGN-
415 to-endosome transport.[44,45] There are two GGA-encoding genes in *S. pombe*,
416 *gga21* and *gga22*, which play partially redundant roles.[45] Cw9pi remained non-
417 toxic in single deletion mutants lacking *gga21* or *gga22* (Figures S4A). However,
418 in the *gga21Δ gga22Δ* double deletion mutant, which has a moderate growth
419 defect, the expression of Cw9pi further weakened the growth, indicative of a mild
420 toxicity (Figure S4A).

421 Live cell imaging showed that in *gga21Δ gga22Δ* cells, Cw9pi exhibited mainly
422 a vacuole lumen localization, but a small subset of Cw9pi signals were observed
423 on cytoplasmic puncta outside of vacuoles (Figure S4B). Thus, the loss of Gga21
424 and Gga22 only weakly disturbed the trafficking of Cw9pi, possibly because there
425 are additional trafficking factors promoting the TGN-to-endosome trafficking of
426 Cw9pi. We surmised that partially reducing the ubiquitination of Cw9pi using PY
427 mutations that moderately weaken the in vitro ubiquitination of Cw9pi(1-104) may
428 enhance the phenotypic consequence of losing Gga21 and Gga22. Indeed, Cw9pi-
429 PY2* and Cw9pi-PY1*PY3*, which localize to the vacuole lumen and do not show
430 toxicity in the wild-type background, localized to cytoplasmic puncta and caused
431 strong toxicity in the *gga21Δ gga22Δ* double deletion background (Figures S4B
432 and S4C). Furthermore, their puncta showed partial overlap with the TGN marker
433 Sec72-mCherry (Figure S4D). These findings suggest that ubiquitination-mediated
434 trafficking of Cw9pi from the TGN to the endosome renders it non-toxic. Further
435 supporting this model, ubiquitination-defective Cw9pi-3PY* protein exhibited co-
436 localization with the TGN marker (Figure S4E).
437

438 **Ubiquitination neutralizes the toxicity of antidotes encoded by other *wtf***
439 **genes from *S. pombe* and *S. octosporus***

440 Among the 16 non-pseudo *wtf* genes in the *S. pombe* reference genome,[8] all but
441 the four most divergent genes (*wtf7*, *wtf11*, *wtf14*, and *wtf15*) encode antidotes
442 harboring the PY1 and PY2 motifs (Figure 3A). Our analysis of Cw9pi led us to
443 hypothesize that like Cw9pi, these PY motif-containing antidote proteins may also
444 be kept non-toxic by ubiquitination. This model predicts that artificially preventing
445 ubiquitination of these antidote proteins may release their toxicity. To test this idea,
446 we applied the DUB tethering analysis on the antidote products of these 16 non-
447 pseudo *wtf* genes.

448 We crossed a strain expressing a GFP-tagged antidote protein from a thiamine-
449 repressible promoter to a strain expressing GBP-DUB or a strain expressing GBP-
450 DUB* (catalytically dead DUB) on mating/sporulation media containing thiamine
451 and performed tetrad dissection analysis on media lacking thiamine. Spore
452 progeny harboring both the *GFP-antidote* allele and the *GBP-DUB* allele were
453 inviable for nine *wtf* genes, including all four genes that can express both the
454 antidote and the poison (*wtf4*, *wtf13*, *wtf19,* and *wtf23*) and five genes that can only
455 express the antidote (*wtf9*, *wtf10*, *wtf16*, *wtf18*, and *wtf21*) (Figure 6A). For the
456 antidote-only gene *wtf25*, spore progeny of the *GFP-antidote GBP-DUB* genotype
457 formed only extremely small colonies. Antidotes encoded by the other six non-
458 pseudo *wtf* genes (*wtf5*, *wtf20*, and the four divergent genes) did not show toxicity
459 upon DUB tethering (Figure S5A). For all 16 *wtf* genes, combining the *GFP-*
460 *antidote* allele with the *GBP-DUB** allele did not result in spore viability loss or
461 growth defect (Figures 6A and S5A). These results indicate that PY motif-
462 containing antidotes mostly possess intrinsic toxicity that needs to be neutralized
463 by ubiquitination to avoid suicidal killing.

464 The protein products of two antidote-only genes *wtf5* and *wtf10* are 82.9%

465 identical in their amino acid sequences (Figure S5B). However, only Wtf10 but not
466 Wtf5 displayed toxicity in the DUB tethering analysis. To understand the reason
467 behind this difference, we performed sequence swapping between Wtf5 and Wtf10,
468 and found that the difference is determined by the Wtf5(73-142) region (Figure
469 S5C). Within this region, these two proteins only differ at two residues (Figure S5B).
470 Replacing either residue in Wtf5 with the residue in Wtf10 rendered Wtf5 toxic in
471 the DUB tethering analysis (Figure S5D). Thus, Wtf5 may have only recently lost
472 its intrinsic toxicity and can regain the toxicity through a single point mutation.

473 *wtf* genes are present not only in *S. pombe* but also in three other fission yeast
474 species, *S. octosporus*, *S. osmophilus*, and *S. cryophilus*, which diverged from *S.*
475 *pombe* about 100 million years ago.[3] Inspecting sequence alignments of proteins
476 encoded by intact *wtf* genes in these three species showed that the N-terminal
477 cytosolic tails of the antidote isoforms all contain a single conserved PY motif
478 (Figure S6A). We predicted that, like the situation in *S. pombe*, these PY motif-
479 containing antidotes are intrinsically toxic and are kept non-toxic by ubiquitination.
480 To test this idea, we applied the DUB tethering analysis by crossing *S. pombe*
481 strains expressing individually GFP-tagged antidotes of four *S. octosporus wtf*
482 genes (*octo_wtf14*, *octo_wtf21*, *octo_wtf25*, and *octo_wtf46*) to an *S. pombe* strain
483 expressing GBP-DUB. Cross progeny harboring both the *GFP-octo_antidote* allele
484 and the *GBP-DUB* allele were inviable (Figure 6B). These results suggest that
485 ubiquitination-mediated toxicity neutralization is an ancient mechanism dating
486 back to the common ancestors of *wtf* genes existing 100 million years ago.

487

488 Discussion

489 Our study uncovers a ubiquitination-mediated toxicity neutralization mechanism
490 employed by *wtf* KMDs to convert the intrinsically toxic long isoform product into a
491 non-toxic antidote (Figure 6C). This conversion requires conserved PY motifs,

492 which promote ubiquitination through binding Rsp5/NEDD4 family ubiquitin ligases.
493 Ubiquitination serves as a sorting signal to direct the trafficking of the antidote
494 protein from the TGN to the endosome, and thereby prevents it from exerting toxic
495 effects at the TGN and/or at non-endosomal post-TGN locations. The ability of the
496 antidote to interact with the poison allows the antidote to target the poison to the
497 endosome and thereby neutralize the toxicity of the poison.

498 It remains unclear how non-ubiquitinated Wtf proteins cause toxicity. The partial
499 co-localization of the toxic forms of Cw9 with a TGN marker suggests a possibility
500 that the toxicity is due to perturbation of TGN functions, but we cannot rule out the
501 possibility that toxicity is exerted at non-endosomal post-Golgi membrane
502 locations. It has been proposed that the cytoplasmic puncta formed by the poison
503 product of *Sk wtf4* are protein aggregates.[5] In this study, we show that Cw9ki is a
504 transmembrane protein that traffics through the secretory pathway from the ER to
505 the TGN, where it exhibits a punctate localization pattern, presumably because
506 that is how the TGN appears in light microscopy.

507 The mechanisms uncovered in this study can serve as a paradigm for
508 understanding how poison-antidote duality of single-gene KMDs is generated. We
509 propose that for single-gene KMDs, ubiquitination or other types of post-
510 translational modifications may be a commonly employed mechanism for
511 converting a toxic protein product to a non-toxic protein or converting a non-toxic
512 protein product to a toxic protein. As a result, both a toxic protein and a non-toxic
513 protein can be produced from the same gene. An advantage of such a mechanism
514 is that at the amino acid sequence level, post-translational modifications can be
515 determined by simply a short sequence motif such a single PY motif. Interestingly,
516 we noticed that another single-gene KMD family, the *Spk-1* gene and its homologs
517 in *Neurospora*,[9] encode transmembrane proteins containing a conserved PY motif
518 (Figure S6B), suggesting the possibility that PY motif-mediated ubiquitination may

519 control the poison-antidote duality of *Spk-1* family KMDs.

520 For single-gene KMDs that, like *wtf* driver genes, express overlapping but non-
521 identical protein products, post-translational modification-based poison-antidote
522 duality can be achieved through the presence of modification determinant
523 sequence motif(s) in the product-specific amino acid sequence. For single-gene
524 KMDs that express a single polypeptide, post-translational modification-based
525 poison-antidote duality may be realized through variable activities of
526 modifying/demodifying enzymes. For example, a modifying enzyme whose activity
527 is up-regulated in spores may prevent the toxicity of the newly synthesized KMD
528 product in spores and allow it to detoxify the poison inherited from the zygote.

529 For the non-toxic protein product of a single-gene KMD to fulfill the role of the
530 antidote, it needs to exert a toxicity neutralizing activity on the poison product. As
531 shown here for the case of *cw9*, this need can be satisfied if the poison and the
532 antidote can interact with each other. As the poison and antidote products of a
533 single-gene KMD share an overlapping region, the poison-antidote interaction can
534 be achieved if the overlapping region is capable of self-interaction.

535 Summing up the above considerations, we propose that poison-antidote duality
536 of single-gene KMDs can be based on the concurrent presence of the following
537 two features: 1) The gene product(s) can engage in homotypic interactions; and 2)
538 At least one gene product isoform undergoes a post-translational modification that
539 either causes or prevents toxicity. This model has implications for the evolutionary
540 origin of single-gene poison-antidote KMDs. We envision that any preexisting
541 genes encoding self-interacting proteins regulated by a post-translational
542 modification are potential precursors of single-gene poison-antidote KMDs. Should
543 a mutation arise that renders such a protein toxic in either the unmodified or
544 modified form, but not both, a rudimentary KMD may emerge. Subsequent
545 evolutionary processes would then refine its selfish behavior, ultimately

546 culminating in the formation of a fully-developed meiotic driver gene.

547

548 Acknowledgments

549 We thank Dan Zhao for providing a plasmid containing the *P81nmt1a* promoter;
550 Yan Ding for assistance with the in vitro ubiquitination assay; Gaihong Cai and She
551 Chen for assistance with the mass spectrometry analysis; and Ping Wei for
552 providing *S. cerevisiae* plasmids. This work was supported by grants from the
553 Ministry of Science and Technology of the People's Republic of China and the
554 Beijing municipal government.

555

556 Author Contributions

557 Conceptualization: J.-X.Z. and L.-L.D.; Methodology and Investigation: J.-X.Z., T.-
558 Y.D., G.-C.S., Z.-H.M., Z.-D.J., W.H., F.S., W.H., M.-Q.D., L.-L.D.; Writing – Original
559 Draft: J.-X.Z. and L.-L.D.; Writing – Review and Editing: J.-X.Z. and L.-L.D.

560

561 Declaration of Interests

562 The authors declare no competing interests.

563

564

565 METHODS

566 Strains and plasmids

567 Yeast strains used in this study are listed in Table S1, and plasmids used in this
568 study are listed in Table S2. Strain construction methods and media used for *S.*
569 *pombe* culturing are as described.[46,47] The SC medium (FunGenome, Beijing,
570 China) was used for culturing *S. cerevisiae*. Deletion strains were created using
571 PCR-based gene deletion. Strains expressing proteins fused with various tags

572 from native promoters were created using PCR-based tagging. Plasmids carrying
573 the *Pnmt1*, *P41nmt1*, or *P81nmt1* promoter were based on modified pDUAL
574 vectors.[48,49] The DUB used in the DUB tethering analysis consists of a linker region
575 from the budding yeast Ubp7 (residues 561-591) and the catalytic domain from the
576 herpes simplex virus 1 (HSV-1) UL36 protein (residues 15-260).[33,34] The
577 catalytically dead DUB* harbors a C40S mutation in the sequence of UL36. The
578 *P81nmt1a* promoter was constructed by inserting a 57 bp sequence that contains
579 the restriction sites of XhoI, SalI, NruI, AscI, PstI, and ApaI between the NheI and
580 BamHI sites downstream of the *P81nmt1* promoter.[50] Plasmids containing the
581 *PtetO7* promoter were constructed by replacing the *Pnmt1* promoter of the pDUAL
582 vector. For the plasmid expressing Sar1-T34N, the PCR sequence was inserted
583 into the modified pSIV vector.[51] *cw9ki-only* corresponds to the Te form of *cw9*
584 reported in the previous study.[8] Other forms of *cw9* used in this study were
585 generated by PCR-based plasmid construction. Plasmids expressing proteins in
586 budding yeast under the control of the *pGAL1* promoter were constructed using
587 pRS305 vectors.[52] Plasmids expressing proteins in budding yeast under the
588 control of the *pCYC1*, *pTEF1*, and *pURA3* promoters were constructed using
589 pNH605 vectors.[52] For the doxycycline (DOX) inducible system in budding yeast,
590 the sequence of *cw9ki* was inserted downstream of the *pTETO7* promoter, and the
591 plasmid expressing rtTA-Msn2 was constructed with the pNH607 vector.[52]
592 Plasmids expressing different fragments of Cw9pi and truncated Pub1/Pub3 were
593 constructed by inserting coding sequences into pETDuet vectors or pET15b
594 vectors. Plasmids expressing Uba1, Ubc4, and ubiquitin in *E. coli* were obtained
595 from the previous study.[53]
596
597 **Tetrad analysis**
598 Haploid parental strains freshly grown on YES plates were mixed and spotted on

599 SPAS plates. The SPAS plates were incubated at 30 °C for about 24 hr. The tetrad
600 analysis was carried out using a TDM50 tetrad dissection microscope (Micro Video
601 Instruments, Avon, USA) and spores were placed on YES plates. For the DUB
602 tethering analysis, thiamine was added to SPAS plates, and spores were placed
603 on PMG plates without thiamine.
604
605 **Spot assay**
606 Log-phase cells grown in the YES medium were washed twice with water and
607 diluted to an OD_{600} of 0.4 in water. 200 μL of cell suspension of each strain was
608 transferred to a well in a 96-well plate. Five-fold serial dilutions of cell suspension
609 were made in the 96-well plate and spotted onto plates using a pin tool (3 mm
610 diameter pins). Plates were incubated at 30 °C for about two days. For strains
611 expressing *cw9* from thiamine-repressible promoters, PMG plates with or without
612 thiamine were used. For *S. pombe* strains expressing *cw9* from the *PtetO7*
613 promoter, MSA plates with or without 2.5 μg/mL of anhydrotetracycline (ahTet)
614 were used.[54] For *S. cerevisiae* strains expressing *cw9* from the *pGAL1* promoter,
615 SC plates with 2% galactose or glucose were used. For *S. cerevisiae* strains
616 expressing *cw9* from the *pTETO7* promoter, SC plates with or without 200 μg/mL
617 of doxycycline (DOX) were used.
618
619 **Protein extraction**
620 Cell lysates were prepared from approximately 3 OD_{600} units of cells using a
621 trichloroacetic acid (TCA) lysis method.[55] The cells were harvested and
622 resuspended in 100 μL of water. Cells were lysed on ice for 15 min by adding 75
623 μL of NaOH/2-mercaptoethanol (1.85 M NaOH, 7.5% (v/v) 2-mercaptoethanol) to
624 the suspension. The proteins were precipitated by adding 75 μL of 55% (w/v) TCA
625 solution for 10 min on ice. After centrifuging the sample at 13000 rpm for 10 min,

626 the supernatant was removed. Following the addition of about 5 μL of neutralizing
627 buffer (1.5 M Tris-HCl, pH 8.8) to prevent any color change, the protein pellet was
628 resuspended in 100 μL of SDS loading buffer (60 mM Tris-HCl, pH 6.8, 4% 2-
629 mercaptoethanol, 4% SDS, 0.01% bromophenol blue, 5% glycerol) at 65 °C for 20
630 min.
631

632 **Immunoprecipitation**

633 About 30 OD_{600} units of cells were harvested. The cells were mixed with 300 μL of
634 lysis buffer (100 mM Tris-HCl, pH 7.5, 50 mM NaCl, 50 mM NaF, 1 mM EDTA, 1
635 mM EGTA, 10% glycerol, 1% Triton X-100, 1 mM DTT, 1 mM PMSF, 1× Roche
636 protease inhibitor cocktail) and about 500 μL of 0.5-mm-diameter glass beads.
637 Using a Fastprep-24 device, bead beating lysis was carried out. The setting was
638 6.5 m/s for 30 s followed by a 2-min on-ice cooling. The beating step was repeated
639 three times to make sure more than 90% of cells were lysed. Microtubes used for
640 bead beating were punctured at the bottom with a hot needle and the lysates were
641 collected into new microtubes by centrifugation at 3000 rpm for 1 min at 4 °C. The
642 cell lysates were cleared by centrifugation at 13000 rpm for 10 min. The
643 supernatants were incubated with GFP-Trap agarose beads for 2 hr at 4 °C.
644 Following incubation, the beads were washed with lysis buffer devoid of DTT,
645 PMSF, and the protease inhibitor cocktail. Bead-bound proteins were eluted by
646 incubating the beads at room temperature with SDS loading buffer for 10 min.
647

648 **Affinity purification coupled with mass spectrometry (AP-MS) analysis**

649 AP-MS analysis was performed as described[34] with some modifications. About
650 1000 OD_{600} units of cells were harvested. Cells were lysed by grinding in liquid
651 nitrogen. The powder was mixed with 30 mL of lysis buffer as described above and
652 incubated for 30 min at 4 °C. After centrifugation, the cell lysate was incubated with

653 GFP-Trap agarose beads for 2 hr at 4 °C. After incubation, the beads were washed
654 four times with lysis buffer. Elution was carried out by incubating the beads at 65 °C
655 with SDS loading buffer. Eluted proteins were separated by SDS-PAGE. Protein
656 bands on the SDS-PAGE gel were de-stained and in-gel digested with sequencing
657 grade trypsin (10 ng/μL trypsin, 50 mM ammonium bicarbonate, pH 8.0) overnight
658 at 37 °C. Peptides were extracted with 5% formic acid/50% acetonitrile and 0.1%
659 formic acid/75% acetonitrile sequentially and then concentrated to about 20 μl. The
660 extracted peptides were separated by an pre-column (75 μm × 5 cm) packed with
661 10 μm spherical C18 reversed phase material (YMC, Kyoyo, Japan) and analytical
662 capillary column (100 μm × 15 cm) packed with 3 μm spherical C18 reversed
663 phase material (Dr. Maisch, GmbH, Germany). A Waters nanoAcquity UPLC
664 system (Waters, Milford, USA) was used to generate the following HPLC gradient:
665 0-8% B in 10 min, 8-30% B in 30 min, 30-80% B in 15 min, 80% B in 5 min (A =
666 0.1% formic acid in water, B = 0.1% formic acid in acetonitrile). The eluted peptides
667 were sprayed into a LTQ Orbitrap Velos mass spectrometer (Thermo Fisher
668 Scientific, San Jose, CA, USA) equipped with a nano-ESI ion source. The mass
669 spectrometer was operated in data-dependent mode with one MS scan followed
670 by ten HCD (High-energy Collisional Dissociation) MS/MS scans for each cycle.
671 With the cutoff of peptide FDR < 1%, proteins were identified using the pFind
672 program.[56]
673

674 **Recombinant protein purification**

675 Recombinant proteins containing the His_6 tag were expressed in *E. coli* BL21 or
676 Rosetta strain. *E. coli* cells were cultured in 200 mL of LB medium (10 g/L
677 bactotryptone, 5 g/L yeast extract, 10 g/L NaCl) containing 50 mg/L of ampicillin.
678 When OD_{600} reached 0.4-0.6, 40 μL of 1 M IPTG was added and the culture was
679 incubated at 16 °C for 18 hr. The following steps were performed at 4 °C or on ice.

680 The cells were harvested and mixed with 8 mL of *E. coli* lysis buffer (50 mM
681 NaH_2PO_4, pH 8.0, 300 mM NaCl, 10 mM imidazole, 10% glycerol). The cell
682 suspension was transferred to a 10 mL beaker, and cells were lysed by sonication.
683 The lysate was centrifuged at 4000 rpm for 10 min at 4 °C. The supernatant was
684 incubated with Ni-NTA beads at 4 °C for 1 hr. The beads were washed three times
685 with wash buffer (50 mM NaH_2PO_4, pH 8.0, 300 mM NaCl, 20 mM imidazole, 10%
686 glycerol). Elution was performed four times by incubating the beads each time with
687 an equal volume of elution buffer (50 mM NaH_2PO_4, pH 8.0, 300 mM NaCl, 250
688 mM imidazole, 10% glycerol). The eluate was stored at −80 °C.
689

690 **GST pulldown**

691 For analyzing the interactions between Cw9pi(1-52) and three E3 ligases (Pub1,
692 Pub2, and Pub3) and the interactions between Cw9pi N-terminal fragments and
693 Pub3, the E3 ligases were expressed in *S. pombe* and Cw9pi fragments were
694 expressed in *E. coli*. *S. pombe* lysates were generated the same way as in the
695 immunoprecipitation analysis. *E. coli* lysates were generated the same way as in
696 recombinant protein purification, except for the composition of the lysis buffer (50
697 mM phosphate buffer, pH 7.4, 200 mM NaCl, 10% glycerol, 0.05% NP-40). After
698 centrifugation, 1 mL of *E. coli* lysate and 100 μL of *S. pombe* lysate were mixed
699 and incubated at 4 °C for 30 min before the addition of glutathione-sepharose
700 beads. After 2-hour incubation, the beads were washed four times with *E. coli* lysis
701 buffer and subsequently eluted with SDS loading buffer.
702 For the interactions between Cw9pi N-terminal fragments and Pub1-ΔC2,
703 proteins were all expressed in *E. coli* and the other steps were as described above.
704

705 **In vitro ubiquitination**

706 In vitro ubiquitination was performed as described[31] with some modifications. Mix

707 1 was prepared as follows: 4 μL of buffer A (50 mM Tris-HCl, pH 7.5, 100 mM NaCl,
708 10% glycerol), 2 μL of 5 × ATP (10 mM ATP, 50 mM $MgCl_2$, 5 mM DTT in buffer A),
709 1 μL of Uba1 (0.1 μg), 1 μL of Ubc4 (2.5 μg), 2 μL of ubiquitin (7 μg). Mix 1 was
710 preincubated for 10 min at 25 °C. Mix 2 was prepared as follows: 6.5 μL of buffer
711 A, 2 μL of 5 × ATP, 0.5 μL of Pub1 (0.3 μg), 1 μL of Cw9pi N-terminal fragment (2
712 μg) as the substrate protein, which was fused to eight copies of a modified myc
713 tag lacking lysine (myc*: EQRLISEEDL).[57] Mix 1 was added to Mix 2 and incubated
714 for 3 hr at 25 °C. The reaction was stopped by adding SDS loading buffer. During
715 immunoblotting, immediately after the protein transfer step, the PVDF membrane
716 was treated for 30 min with 1% glutaraldehyde in PBS to render the transferred
717 proteins more tightly associated with the membrane.[58]
718
719 **In vitro ubiquitination coupled with mass spectrometry analysis**
720 For in vitro ubiquitination followed by MS analysis, 10 μg of the substrate, 0.5 μg
721 of Uba1, and 0.5 μg of Pub1/Pub3 were used. The ubiquitination reaction was
722 carried out at 25 °C overnight. $CaCl_2$ was added to a final concentration of 1 mM.
723 The samples were digested with trypsin overnight at 37 °C. Formic acid was added
724 to the final concentration of 5% to stop the digestion reaction. LC-MS/MS analysis
725 was performed on an Easy-nLC 1000 II HPLC instrument (Thermo Fisher Scientific,
726 San Jose, CA, USA) coupled to an Orbitrap QE-HF mass spectrometer (Thermo
727 Fisher Scientific, San Jose, CA, USA). Peptides were loaded on a pre-column (100
728 μm ID, 4 cm long, packed with C18 10 μm 120 Å resin from YMC Co., Ltd) and
729 separated on an analytical column (75 μm ID, 10 cm long, packed with Luna C18
730 1.8 μm 100 Å resin from Welch Materials) using an acetonitrile gradient from 0%
731 to 30% in 70 min at a flow rate of 250 nL/min. The top 20 intense precursor ions
732 from each full scan (resolution 60000) were isolated for higher-energy collisional
733 dissociation tandem mass spectrometry spectra analysis (HCD MS2; normalized

734 collision energy 27) with a dynamic exclusion time of 45 s. Tandem mass
735 spectrometry fragment ions were detected using orbitrap in a normal scan mode.
736 The pFind software was used to identify proteins with the cutoff of peptide FDR <
737 1%.
738

739 **Streptavidin pulldown of biotin-tagged ubiquitin**

740 About 30 OD_{600} units of *S. pombe* cells were harvested. Cells were resuspended
741 with 500 μL of water and incubated at room temperature for 10 min after the
742 addition of 500 μL of 0.7 M NaOH. After centrifugation, the supernatants were
743 discarded. The pellets were resuspended with 1 mL of lysis buffer (2% SDS, 60
744 mM Tris-HCl, pH 6.8, 5% glycerol, 4% 2-mercaptoethanol) and incubated at 42 °C
745 for 20 min. After centrifugation, the supernatants were incubated with 20 μL of high
746 capacity streptavidin agarose (Thermo Fisher Scientific, San Jose, CA, USA) at
747 room temperature for 3 hr. After incubation, the beads were washed two times with
748 wash buffer A (50 mM Tris-HCl, pH 7.5, 150 mM NaCl, 1 mM EDTA, 1mM EGTA,
749 1% Triton X-100, 0.4% SDS, 1% NP-40, 1× Roche protease inhibitor cocktail), one
750 time with wash buffer B (50 mM Tris-HCl, pH 7.5, 2% SDS), and two times with
751 wash buffer A. Elution was performed two times by incubating the beads each time
752 with 20 μL of elution buffer (50 mM Tris-HCl, pH 8.0, 2% SDS, 5 mM biotin) at
753 60 °C for 20 min.
754

755 **Electron microscopy**

756 Approximately 20 OD_{600} units of cells treated with 2.5 μg/mL ahTet for 6 hr were
757 harvested, and then washed once with water. Cells was fixed with freshly prepared
758 1% glutaraldehyde and 4% KMnO4, and then dehydrated through a graded
759 ethanol series and embedded in Spurr's resin.[59] An FEI Tecnai G2 Spirit electron
760 microscope operating at 120kV with a 4k×4k Gatan 895 CCD camera was used to

761 examine thin sections.

762

763 **Fluorescence microscopy**

764 For imaging of vegetative cells expressing Cw9 from a thiamine-repressible
765 promoter, cells were first cultured in the YES medium, which contains thiamine.
766 Log-phase cells were harvested and washed two times with the EMM medium,
767 which lacks thiamine. Next, cells were cultured in the EMM medium to induce
768 protein expression. For imaging of spores, we crossed the two haploid strains on
769 the SPAS plates. The SPAS plates were incubated at 30 °C for about 24 hr. Cells
770 were scraped from the SPAS plates and placed onto slides for imaging.

771 Images shown in Figures 1D, S1B, 5A, 5C, 5E, 5F, 5G, S3H, and S3I were
772 obtained using a DeltaVision PersonalDV system (Applied Precision) equipped
773 with an mCherry/YFP/CFP filter set (Chroma 89006 set) and a Photometrics
774 Evolve 512 EMCCD camera. The SoftWoRx program was used to analyze the
775 images. Images shown in Figures 5K, S3C, S3D, S3G, S3J, S4B, S4D, and S4E
776 were obtained using an Andor Dragonfly 200 high speed confocal microscope
777 system equipped with a Sona sCMOS camera. Images were acquired using the
778 Fusion software and analyzed using Fiji. During image analysis, we specifically
779 opted to select cells that exhibited no obvious depressions, as those with such
780 features were found to attenuate the fluorescence emission from mECitrine^{int}-
781 Cw9ki.

782

783 **Protein sequence alignment**

784 For the sequence alignment shown in Figure 3A, the N-terminal cytosolic tails of
785 Cw9pi, Cw27pi, and Wtf proteins encoded by the 16 intact *wtf* genes in the
786 reference *S. pombe* genome were analyzed. The ranges of the N-terminal
787 cytosolic tails were based on the transmembrane topology predicted by TOPCONS

788 (https://topcons.cbr.su.se/)[60] for the four divergent Wtf proteins (Wtf7, Wtf11, Wtf14,
789 and Wtf15), and the transmembrane topology described in our previous study for
790 the other 14 proteins.[8] Sequence alignment was performed using the MAFFT web
791 server (https://mafft.cbrc.jp/alignment/server/) with the L-INS-i algorithm.[61,62]
792 For the sequence alignment shown in Figure S6A, the long isoform protein
793 sequences of 30 intact *wtf* genes from *S. osmophilus*,[63] 48 intact *wtf* genes from
794 *S. octosporus*,[3] and 2 intact *wtf* genes from *S. cryophilus*[3] were analyzed using
795 MAFFT. The transmembrane helices of these Wtf proteins were predicted using
796 PolyPhobius (http://phobius.sbc.su.se/poly.html).[64] Only the N-terminal cytosolic
797 tails were shown in Figure S6A. The sequence alignment shown in Figure S6B
798 was based on a published alignment.[9]
799
800
801 **References**

802 1. Núñez, M. A. B., Nuckolls, N. L. & Zanders, S. E. (2018). Genetic villains: killer meiotic drivers. *Trends*
803 *Genet.* **34**, 424-433, 10.1016/j.tig.2018.02.003.
804 2. Nuckolls, N. L., Nidamangala Srinivasa, A., Mok, A. C., Helston, R. M., Bravo Núñez, M. A., Lange, J.
805 J., Gallagher, T. J., Seidel, C. W. & Zanders, S. E. (2022). S. pombe wtf drivers use dual transcriptional
806 regulation and selective protein exclusion from spores to cause meiotic drive. *PLoS Genet.* **18**,
807 e1009847, 10.1371/journal.pgen.1009847.
808 3. De Carvalho, M., Jia, G.-S., Srinivasa, A. N., Billmyre, R. B., Xu, Y.-H., Lange, J. J., Sabbarini, I. M., Du,
809 L.-L. & Zanders, S. E. (2022). The wtf meiotic driver gene family has unexpectedly persisted for over
810 100 million years. *eLife* **11**, e81149, 10.7554/eLife.81149.
811 4. Núñez, M. A. B., Sabbarini, I. M., Eickbush, M. T., Liang, Y., Lange, J. J., Kent, A. M. & Zanders, S. E.
812 (2020). Dramatically diverse Schizosaccharomyces pombe wtf meiotic drivers all display high
813 gamete-killing efficiency. *PLoS Genet.* **16**, e1008350, 10.1371/journal.pgen.1008350.
814 5. Nuckolls, N. L., Mok, A. C., Lange, J. J., Yi, K., Kandola, T. S., Hunn, A. M., McCroskey, S., Snyder, J. L.,
815 Núñez, M. A. B. & McClain, M. (2020). The wtf4 meiotic driver utilizes controlled protein
816 aggregation to generate selective cell death. *eLife* **9**, e55694, 10.7554/eLife.55694.
817 6. Núñez, M. A. B., Lange, J. J. & Zanders, S. E. (2018). A suppressor of a wtf poison-antidote meiotic
818 driver acts via mimicry of the driver's antidote. *PLoS Genet.* **14**, e1007836,
819 10.1371/journal.pgen.1007836.
820 7. Nuckolls, N. L., Núñez, M. A. B., Eickbush, M. T., Young, J. M., Lange, J. J., Jonathan, S. Y., Smith, G.
821 R., Jaspersen, S. L., Malik, H. S. & Zanders, S. E. (2017). wtf genes are prolific dual poison-antidote

822 meiotic drivers. *eLife* **6**, e26033, 10.7554/eLife.26033.
823 8. Hu, W., Jiang, Z.-D., Suo, F., Zheng, J.-X., He, W.-Z. & Du, L.-L. (2017). A large gene family in fission
824 yeast encodes spore killers that subvert Mendel's law. *eLife* **6**, e26057, 10.7554/eLife.26057.
825 9. Svedberg, J., Vogan, A. A., Rhoades, N. A., Sarmarajeewa, D., Jacobson, D. J., Lascoux, M., Hammond,
826 T. M. & Johannesson, H. (2021). An introgressed gene causes meiotic drive in Neurospora sitophila.
827 *Proc. Natl. Acad. Sci. U.S.A.* **118**, 10.1073/pnas.2026605118.
828 10. Zanders, S. & Johannesson, H. (2021). Molecular mechanisms and evolutionary consequences of
829 spore killers in ascomycetes. *Microbiol. Mol. Biol. Rev.* **85**, e00016-00021, 10.1128/MMBR.00016-
830 21.
831 11. Vogan, A. A., Martinossi-Allibert, I., Ament-Velásquez, S. L., Svedberg, J. & Johannesson, H. (2022).
832 The spore killers, fungal meiotic driver elements. *Mycologia* **114**, 1-23,
833 10.1080/00275514.2021.1994815.
834 12. Saupe, S. J. & Johannesson, H. (2022). On the Mechanistic Basis of Killer Meiotic Drive in Fungi.
835 *Annu. Rev. Microbiol.* **76**, 305-323, 10.1146/annurev-micro-041320-113730.
836 13. Grognet, P., Lalucque, H., Malagnac, F. & Silar, P. (2014). Genes that bias Mendelian segregation.
837 *PLoS Genet.* **10**, e1004387, 10.1371/journal.pgen.1004387.
838 14. Vogan, A. A., Ament-Velásquez, S. L., Granger-Farbos, A., Svedberg, J., Bastiaans, E., Debets, A. J.,
839 Coustou, V., Yvanne, H., Clavé, C. & Saupe, S. J. (2019). Combinations of Spok genes create multiple
840 meiotic drivers in Podospora. *eLife* **8**, e46454, 10.7554/eLife.46454.
841 15. Bowen, N. J., Jordan, I. K., Epstein, J. A., Wood, V. & Levin, H. L. (2003). Retrotransposons and their
842 recognition of pol II promoters: a comprehensive survey of the transposable elements from the
843 complete genome sequence of Schizosaccharomyces pombe. *Genome Res.* **13**, 1984-1997,
844 10.1101/gr.1191603.
845 16. Basi, G., Schmid, E. & Maundrell, K. (1993). TATA box mutations in the Schizosaccharomyces pombe
846 nmt1 promoter affect transcription efficiency but not the transcription start point or thiamine
847 repressibility. *Gene* **123**, 131-136, 10.1016/0378-1119(93)90552-e.
848 17. Zilio, N., Wehrkamp-Richter, S. & Boddy, M. N. (2012). A new versatile system for rapid control of
849 gene expression in the fission yeast Schizosaccharomyces pombe. *Yeast* **29**, 425-434,
850 10.1002/yea.2920.
851 18. Chen, Y.-h., Wang, G.-y., Hao, H.-c., Chao, C.-j., Wang, Y. & Jin, Q.-w. (2017). Facile manipulation of
852 protein localization in fission yeast through binding of GFP-binding protein to GFP. *J. Cell Sci.* **130**,
853 1003-1015, 10.1242/jcs.198457.
854 19. Rothbauer, U., Zolghadr, K., Tillib, S., Nowak, D., Schermelleh, L., Gahl, A., Backmann, N., Conrath,
855 K., Muyldermans, S. & Cardoso, M. C. (2006). Targeting and tracing antigens in live cells with
856 fluorescent nanobodies. *Nat. Methods* **3**, 887-889, 10.1038/nmeth953.
857 20. Nefsky, B. & Beach, D. (1996). Pub1 acts as an E6-AP-like protein ubiquitiin ligase in the degradation
858 of cdc25. *EMBO J.* **15**, 1301-1312.
859 21. Tamai, K. K. & Shimoda, C. (2002). The novel HECT-type ubiquitin-protein ligase Pub2p shares
860 partially overlapping function with Pub1p in Schizosaccharomyces pombe. *J. Cell Sci.* **115**, 1847-
861 1857, 10.1242/jcs.115.9.1847.
862 22. Carpy, A., Krug, K., Graf, S., Koch, A., Popic, S., Hauf, S. & Macek, B. (2014). Absolute proteome and

863 phosphoproteome dynamics during the cell cycle of Schizosaccharomyces pombe (Fission Yeast).
864 *Mol. Cell Proteomics* **13**, 1925-1936, 10.1074/mcp.M113.035824.
865 23. Marguerat, S., Schmidt, A., Codlin, S., Chen, W., Aebersold, R. & Bähler, J. (2012). Quantitative
866 analysis of fission yeast transcriptomes and proteomes in proliferating and quiescent cells. *Cell* **151**,
867 671-683, 10.1016/j.cell.2012.09.019.
868 24. Maspero, E., Valentini, E., Mari, S., Cecatiello, V., Soffientini, P., Pasqualato, S. & Polo, S. (2013).
869 Structure of a ubiquitin-loaded HECT ligase reveals the molecular basis for catalytic priming. *Nat.*
870 *Struct. Mol. Biol.* **20**, 696-701, 10.1038/nsmb.2566.
871 25. Staub, O., Dho, S., Henry, P., Correa, J., Ishikawa, T., McGlade, J. & Rotin, D. (1996). WW domains of
872 Nedd4 bind to the proline-rich PY motifs in the epithelial Na+ channel deleted in Liddle's syndrome.
873 *EMBO J.* **15**, 2371-2380.
874 26. Gupta, R., Kus, B., Fladd, C., Wasmuth, J., Tonikian, R., Sidhu, S., Krogan, N. J., Parkinson, J. & Rotin,
875 D. (2007). Ubiquitination screen using protein microarrays for comprehensive identification of Rsp5
876 substrates in yeast. *Mol. Syst. Biol.* **3**, 116, 10.1038/msb4100159.
877 27. Persaud, A., Alberts, P., Amsen, E. M., Xiong, X., Wasmuth, J., Saadon, Z., Fladd, C., Parkinson, J. &
878 Rotin, D. (2009). Comparison of substrate specificity of the ubiquitin ligases Nedd4 and Nedd4-2
879 using proteome arrays. *Mol. Syst. Biol.* **5**, 333, 10.1038/msb.2009.85.
880 28. Henry, P. C., Kanelis, V., O'Brien, M. C., Kim, B., Gautschi, I., Forman-Kay, J., Schild, L. & Rotin, D.
881 (2003). Affinity and specificity of interactions between Nedd4 isoforms and the epithelial Na+
882 channel. *J. Biol. Chem.* **278**, 20019-20028, 10.1074/jbc.M211153200.
883 29. Kanelis, V., Bruce, M. C., Skrynnikov, N. R., Rotin, D. & Forman-Kay, J. D. (2006). Structural
884 determinants for high-affinity binding in a Nedd4 WW3* domain-Comm PY motif complex.
885 *Structure* **14**, 543-553, 10.1016/j.str.2005.11.018.
886 30. Marín, I. (2018). Origin and evolution of fungal HECT ubiquitin ligases. *Sci. Rep.* **8**, 6419,
887 10.1038/s41598-018-24914-x.
888 31. Saeki, Y., Isono, E. & Toh-e, A. (2005). Preparation of ubiquitinated substrates by the PY motif-
889 insertion method for monitoring 26S proteasome activity. *Methods Enzymol.* **399**, 215-227,
890 10.1016/S0076-6879(05)99014-9.
891 32. Kattenhorn, L. M., Korbel, G. A., Kessler, B. M., Spooner, E. & Ploegh, H. L. (2005). A deubiquitinating
892 enzyme encoded by HSV-1 belongs to a family of cysteine proteases that is conserved across the
893 family Herpesviridae. *Mol. Cell* **19**, 547-557, 10.1016/j.molcel.2005.07.003.
894 33. Stringer, D. K. & Piper, R. C. (2011). A single ubiquitin is sufficient for cargo protein entry into MVBs
895 in the absence of ESCRT ubiquitination. *J. Cell Biol.* **192**, 229-242, 10.1083/jcb.201008121.
896 34. Liu, X.-M., Sun, L.-L., Hu, W., Ding, Y.-H., Dong, M.-Q. & Du, L.-L. (2015). ESCRTs cooperate with a
897 selective autophagy receptor to mediate vacuolar targeting of soluble cargos. *Mol. Cell* **59**, 1035-
898 1042, 10.1016/j.molcel.2015.07.034.
899 35. Davidson, R., Laporte, D. & Wu, J.-Q. (2015). Regulation of Rho-GEF Rgf3 by the arrestin Art1 in
900 fission yeast cytokinesis. *Mol. Biol. Cell* **26**, 453-466, 10.1091/mbc.E14-07-1252.
901 36. Cheong, H. & Klionsky, D. J. (2008). Biochemical methods to monitor autophagy-related processes
902 in yeast. *Methods Enzymol.* **451**, 1-26, 10.1016/S0076-6879(08)03201-1.
903 37. Mukaiyama, H., Iwaki, T., Idiris, A. & Takegawa, K. (2011). Processing and maturation of

904 carboxypeptidase Y and alkaline phosphatase in Schizosaccharomyces pombe. *Appl. Microbiol.*
905 *Biotechnol.* **90**, 203-213, 10.1007/s00253-010-3031-3.
906 38. Feyder, S., De Craene, J.-O., Bär, S., Bertazzi, D. L. & Friant, S. (2015). Membrane trafficking in the
907 yeast Saccharomyces cerevisiae model. *Int. J. Mol. Sci.* **16**, 1509-1525, 10.3390/ijms16011509.
908 39. Raiborg, C. & Stenmark, H. (2009). The ESCRT machinery in endosomal sorting of ubiquitylated
909 membrane proteins. *Nature* **458**, 445-452, 10.1038/nature07961.
910 40. Katzmann, D. J., Babst, M. & Emr, S. D. (2001). Ubiquitin-dependent sorting into the multivesicular
911 body pathway requires the function of a conserved endosomal protein sorting complex, ESCRT-I.
912 *Cell* **106**, 145-155, 10.1016/s0092-8674(01)00434-2.
913 41. Tagwerker, C., Flick, K., Cui, M., Guerrero, C., Dou, Y., Auer, B., Baldi, P., Huang, L. & Kaiser, P. (2006).
914 A tandem affinity tag for two-step purification under fully denaturing conditions: application in
915 ubiquitin profiling and protein complex identification combined with in vivocross-linking. *Mol. Cell*
916 *Proteomics* **5**, 737-748, 10.1074/mcp.M500368-MCP200.
917 42. Day, K. J., Casler, J. C. & Glick, B. S. (2018). Budding yeast has a minimal endomembrane system.
918 *Dev. Cell* **44**, 56-72. e54, 10.1016/j.devcel.2017.12.014.
919 43. Connerly, P. L., Esaki, M., Montegna, E. A., Strongin, D. E., Levi, S., Soderholm, J. & Glick, B. S. (2005).
920 Sec16 is a determinant of transitional ER organization. *Curr. Biol.* **15**, 1439-1447,
921 10.1016/j.cub.2005.06.065.
922 44. Pelham, H. R. (2004). Membrane traffic: GGAs sort ubiquitin. *Curr. Biol.* **14**, R357-R359,
923 10.1016/j.cub.2004.04.027.
924 45. Yanguas, F., Moscoso-Romero, E. & Valdivieso, M.-H. (2019). Ent3 and GGA adaptors facilitate
925 diverse anterograde and retrograde trafficking events to and from the prevacuolar endosome. *Sci.*
926 *Rep.* **9**, 1-17, 10.1038/s41598-019-47035-5.
927 46. Forsburg, S. L. & Rhind, N. (2006). Basic methods for fission yeast. *Yeast* **23**, 173-183,
928 10.1002/yea.1347.
929 47. Petersen, J. & Russell, P. (2016). Growth and the environment of Schizosaccharomyces pombe. *Cold*
930 *Spring Harb. Protoc.* **2016**, pdb. top079764, 10.1101/pdb.top079764.
931 48. Matsuyama, A., Shirai, A., Yashiroda, Y., Kamata, A., Horinouchi, S. & Yoshida, M. (2004). pDUAL, a
932 multipurpose, multicopy vector capable of chromosomal integration in fission yeast. *Yeast* **21**,
933 1289-1305, 10.1002/yea.1181.
934 49. Wei, Y., Wang, H.-T., Zhai, Y., Russell, P. & Du, L.-L. (2014). Mdb1, a fission yeast homolog of human
935 MDC1, modulates DNA damage response and mitotic spindle function. *PLoS One* **9**, e97028,
936 10.1371/journal.pone.0097028.
937 50. Belén Moreno, M., Durán, A. & Carlos Ribas, J. (2000). A family of multifunctional thiamine-
938 repressible expression vectors for fission yeast. *Yeast* **16**, 861-872, 10.1002/1097-
939 0061(20000630)16:9<861::AID-YEA577>3.0.CO;2-9.
940 51. Vještica, A., Marek, M., Nkosi, P. J., Merlini, L., Liu, G., Bérard, M., Billault-Chaumartin, I. & Martin,
941 S. G. (2020). A toolbox of stable integration vectors in the fission yeast Schizosaccharomyces pombe.
942 *J. Cell Sci.* **133**, jcs240754, 10.1242/jcs.240754.
943 52. Zhang, Z.-B., Wang, Q.-Y., Ke, Y.-X., Liu, S.-Y., Ju, J.-Q., Lim, W. A., Tang, C. & Wei, P. (2017). Design of
944 tunable oscillatory dynamics in a synthetic NF-κB signaling circuit. *Cell Syst.* **5**, 460-470. e465,

945 10.1016/j.cels.2017.09.016.
946 53. Wei, Y., Diao, L.-X., Lu, S., Wang, H.-T., Suo, F., Dong, M.-Q. & Du, L.-L. (2017). SUMO-targeted DNA
947 translocase Rrp2 protects the genome from Top2-induced DNA damage. *Mol. Cell* **66**, 581-596.
948 e586, 10.1016/j.molcel.2017.04.017.
949 54. Egel, R., Willer, M., Kjærulff, S., Davey, J. & Nielsen, O. (1994). Assessment of pheromone
950 production and response in fission yeast by a halo test of induced sporulation. *Yeast* **10**, 1347-1354,
951 10.1002/yea.320101012.
952 55. Ulrich, H. D. & Davies, A. A. (2009). In vivo detection and characterization of sumoylation targets in
953 Saccharomyces cerevisiae. *Methods Mol. Biol.*, 81-103, 10.1007/978-1-59745-566-4_6.
954 56. Chi, H., Liu, C., Yang, H., Zeng, W.-F., Wu, L., Zhou, W.-J., Wang, R.-M., Niu, X.-N., Ding, Y.-H. & Zhang,
955 Y. (2018). Comprehensive identification of peptides in tandem mass spectra using an efficient open
956 search engine. *Nat. Biotechnol.* **36**, 1059-1061, 10.1038/nbt.4236.
957 57. Golnik, R., Lehmann, A., Kloetzel, P.-M. & Ebstein, F. (2016). Major histocompatibility complex (MHC)
958 class I processing of the NY-ESO-1 antigen is regulated by Rpn10 and Rpn13 proteins and
959 immunoproteasomes following non-lysine ubiquitination. *J. Biol. Chem.* **291**, 8805-8815,
960 10.1074/jbc.M115.705178.
961 58. Okita, N., Higami, Y., Fukai, F., Kobayashi, M., Mitarai, M., Sekiya, T. & Sasaki, T. (2017). Modified
962 Western blotting for insulin and other diabetes-associated peptide hormones. *Sci. Rep.* **7**, 1-11,
963 10.1038/s41598-017-04456-4.
964 59. Kaiser, C. A. & Schekman, R. (1990). Distinct sets of SEC genes govern transport vesicle formation
965 and fusion early in the secretory pathway. *Cell* **61**, 723-733, 10.1016/0092-8674(90)90483-u.
966 60. Tsirigos, K. D., Peters, C., Shu, N., Käll, L. & Elofsson, A. (2015). The TOPCONS web server for
967 consensus prediction of membrane protein topology and signal peptides. *Nucleic Acids Res.* **43**,
968 W401-W407, 10.1093/nar/gkv485.
969 61. Katoh, K., Misawa, K., Kuma, K. i. & Miyata, T. (2002). MAFFT: a novel method for rapid multiple
970 sequence alignment based on fast Fourier transform. *Nucleic Acids Res.* **30**, 3059-3066,
971 10.1093/nar/gkf436.
972 62. Katoh, K. & Standley, D. M. (2013). MAFFT multiple sequence alignment software version 7:
973 improvements in performance and usability. *Mol. Biol. Evol.* **30**, 772-780, 10.1093/molbev/mst010.
974 63. Jia, G. S., Zhang, W. C., Liang, Y., Liu, X. H., Rhind, N., Pidoux, A., Brysch-Herzberg, M. & Du, L. L.
975 (2023). A high-quality reference genome for the fission yeast Schizosaccharomyces osmophilus. *G3*
976 *(Bethesda, Md.)*, 10.1093/g3journal/jkad028.
977 64. Käll, L., Krogh, A. & Sonnhammer, E. L. (2005). An HMM posterior decoder for sequence feature
978 prediction that includes homology information. *Bioinformatics* **21**, i251-i257,
979 10.1093/bioinformatics/bti1014.
980 65. Omasits, U., Ahrens, C. H., Müller, S. & Wollscheid, B. (2014). Protter: interactive protein feature
981 visualization and integration with experimental proteomic data. *Bioinformatics* **30**, 884-886,
982 10.1093/bioinformatics/btt607.

983

984

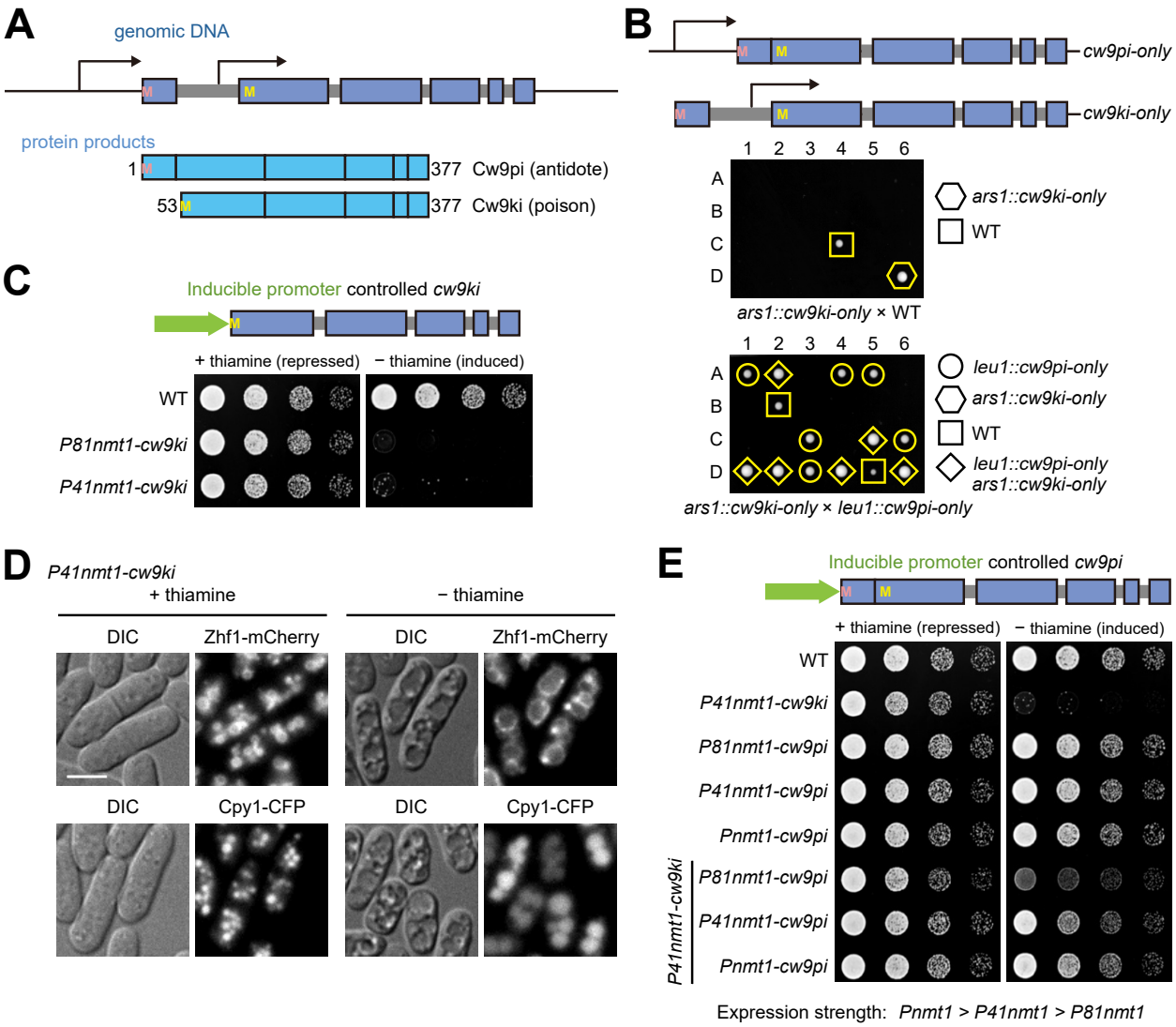

Figure 1. Both the poison product and the antidote product of *cw9* are active in vegetative *S. pombe* cells.

(A) Diagrams depicting the two isoforms encoded by *cw9*. For the diagram of the genomic DNA (top), coding exons are denoted by boxes and introns are denoted by thick grey lines. Transcriptional start sites are shown as bent arrows. Start codons are denoted by the letter M. For the diagram of the protein products (bottom), regions corresponding to the exons are indicated by boxes and the numbering of amino acids is based on the sequence of Cw9pi.

(B) Tetrad analysis showed that a *cw9ki-only* allele inserted at the *ars1* locus on chromosome I killed nearly all spores in a hemizygous cross and a *cw9pi-only* allele inserted at the *leu1* locus on chromosome II neutralized the spore killing effect of *cw9ki-only*. The four spores of each tetrad are labeled A, B, C, and D.

(C) Cw9ki expressed in vegetative *S. pombe* cells from inducible promoters caused toxicity.
(D) Expressing Cw9ki in vegetative *S. pombe* cells from an inducible promoter caused vacuole enlargement. Zhf1 is a vacuole membrane marker. Cpy1 is a vacuole lumen marker. DIC, differential interference contrast. Bar, 5 μm.
(E) Cw9pi expressed in vegetative *S. pombe* cells from inducible promoters neutralized the toxicity of Cw9ki in a dose-dependent manner.

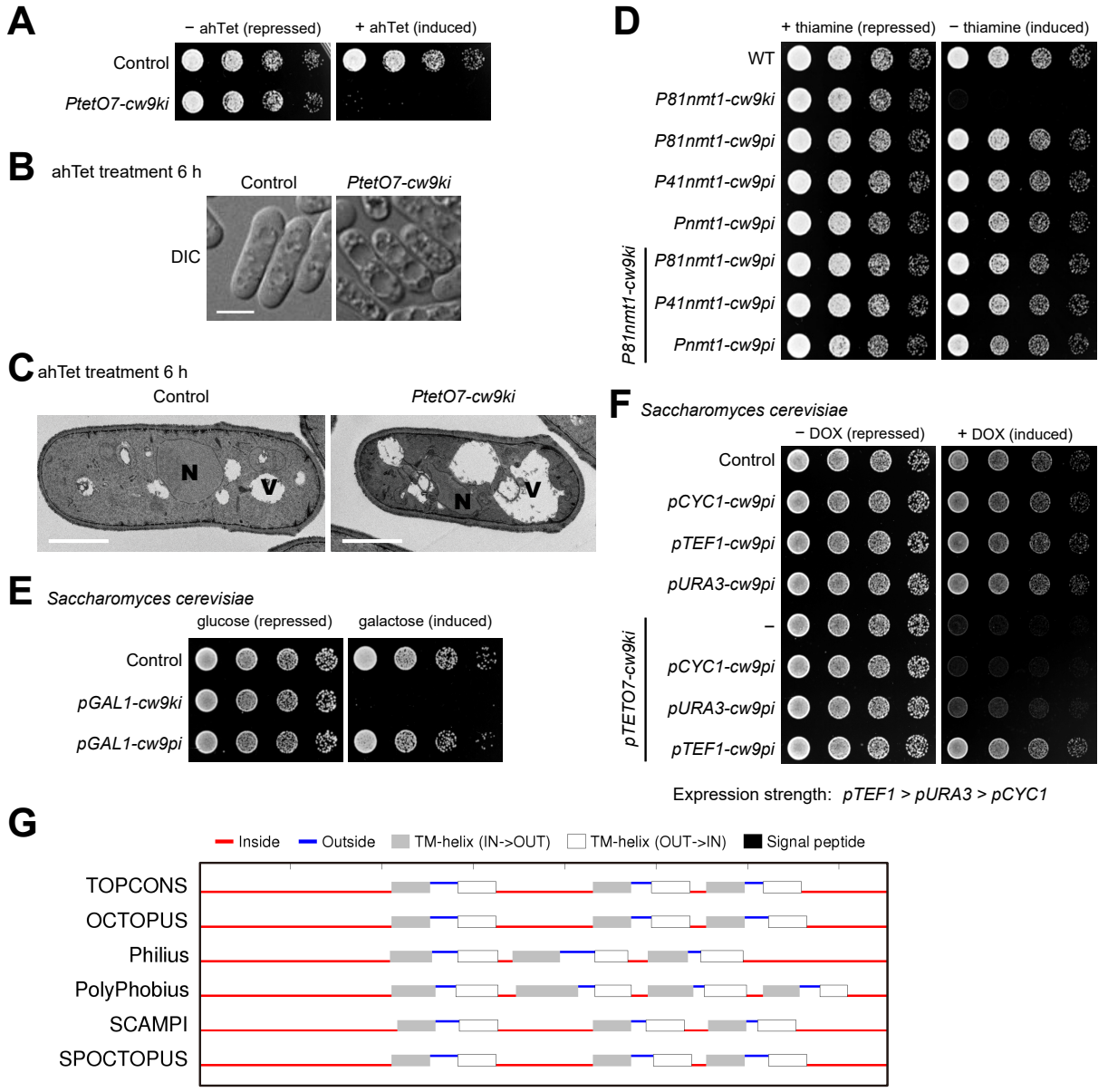

Figure S1. Related to Figure 1 and Figure 2.

(A) Cw9ki expressed from the *PtetO7* promoter caused toxicity in vegetative *S. pombe* cells.

(B) Cw9ki expressed from the *PtetO7* promoter caused vacuole enlargement in vegetative *S. pombe* cells. DIC, differential interference contrast. Bar, 5 μm.

(C) Electron microscopy images of control cells containing an empty vector and cells expressing Cw9ki from the *PtetO7* promoter. N, nucleus; V, vacuole. Bar, 2 μm.

(D) Cw9pi neutralized the toxicity of Cw9ki expressed from the *P81nmt1* promoter.

(E) Cw9ki was toxic to vegetative *S. cerevisiae* cells. *pGAL1* is a galactose-inducible promoter.

(F) Cw9pi neutralized the toxicity of Cw9ki in a dose-dependent manner in *S. cerevisiae*. *pTETO7* promoter is a doxycycline (DOX)-inducible promoter and *pTEF1*, *pURA3*, and *pCYC1* are three constitutive promoters with different strengths.
(G) Transmembrane topology of Cw9pi was predicted using the TOPCONS web server (https://topcons.cbr.su.se/pred/). TOPCONS is a consensus-based method integrating the results of five different topology prediction algorithms. The topology predictions using the individual methods and the consensus prediction of TOPCONS 2.0 are shown. Inside indicates the cytosolic side of the membrane and outside indicates the non-cytosoilic side of the membrane.

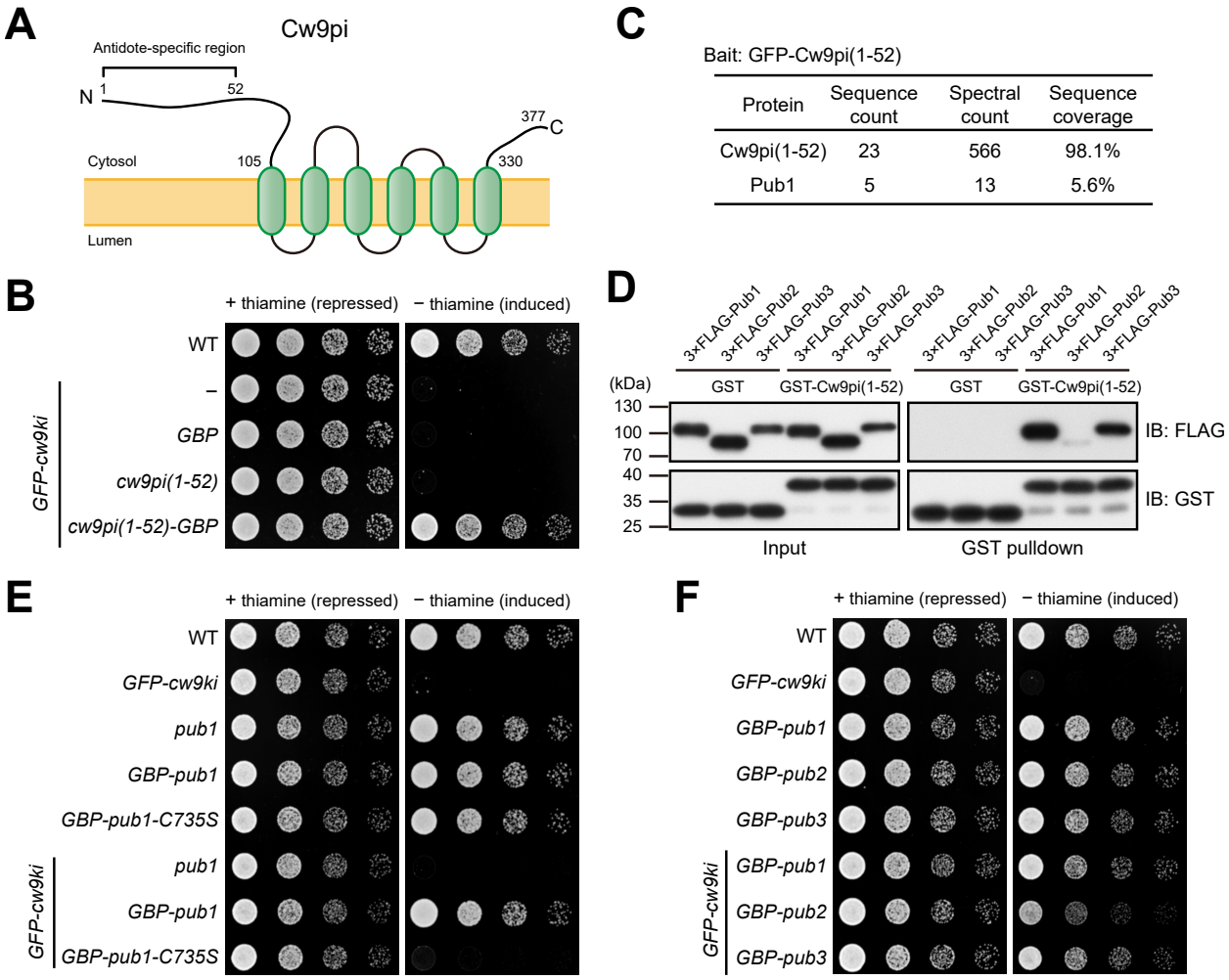

Figure 2. The antidote-specific region of Cw9pi functions as a binding module for the Rsp5/NEDD4 family ubiquitin ligases Pub1 and Pub3.

(A) A diagram depicting the TOPCONS-predicted membrane topology of Cw9pi (see Figure S1G). The antidote-specific region is indicated by the bracket.

(B) The antidote-specific region of Cw9pi, Cw9pi(1-52), when tethered to Cw9ki through the interaction between GFP and the GFP-binding protein (GBP), neutralized the toxicity of Cw9ki. GFP-Cw9ki was expressed from the *P81nmt1* promoter. GBP, Cw9pi(1-52), and Cw9pi(1-52)-GBP were expressed from the *P41nmt1* promoter.

(C) Pub1 co-purified with GFP-Cw9pi(1-52). GFP-Cw9pi(1-52) was purified using GFP-Trap beads. Co-purified proteins were identified by mass spectrometry.

(D) GST pulldown assay showed that Pub1 and Pub3 but not Pub2 can strongly interact with Cw9pi(1-52). The lysate of *S. pombe* cells expressing 3×FLAG-tagged Pub1, Pub2, or Pub3 was mixed with the lysate of *E. coli* cells expressing GST or GST-tagged Cw9pi(1-52) and pulldown was performed using glutathione beads.

(E) Artificial tethering of Pub1 to Cw9ki neutralized the toxicity of Cw9ki. GFP-Cw9ki was expressed from the *P81nmt1* promoter. GBP-Pub1 was expressed from the *P41nmt1* promoter. Pub1-C735S is a catalytically inactive mutant of Pub1.
(F) Tethering Pub1 or Pub3 to Cw9ki confers a strong toxicity neutralization, whereas tethering Pub2 confers a weak toxicity neutralization. GFP-Cw9ki was expressed from the *P81nmt1* promoter. GBP-tagged Pub proteins were expressed from the *P41nmt1* promoter.

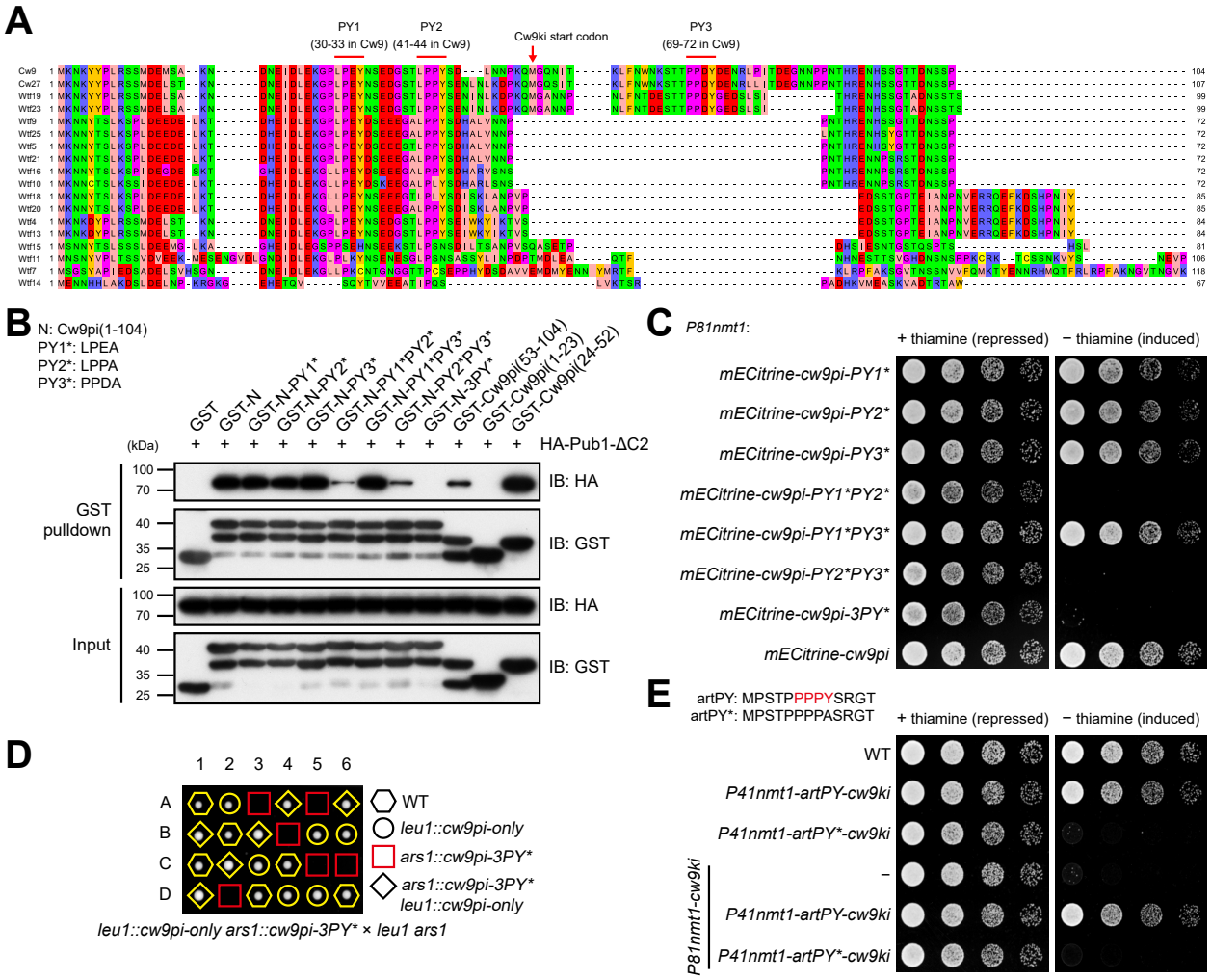

Figure 3. PY motifs in the N-terminal cytosolic tail of Cw9pi mediate Pub1 binding and prevent Cw9pi from becoming toxic.

(A) Multiple sequence alignment of the N-terminal cytosolic tails of the antidote products of 18 *wtf* genes. Three PY motifs in Cw9pi are highlighted.

(B) GST pulldown assay showed that PY motifs in the N-terminal cytosolic tail of Cw9pi are redundantly required for Pub1 binding. Lysates of *E. coli* cells expressing GST-tagged Cw9pi N-terminal fragments were mixed with recombinant 6xHis-HA-Pub1-ΔC2 and pulldown was performed using glutathione beads. N denotes Cw9pi(1-104). Asterisk denotes the Y-to-A mutation in the PY motif.

(C) PY motif mutations strongly diminishing Pub1 binding rendered Cw9pi toxic to vegetative cells.

(D) Cw9pi-3PY* under the control of the native promoter caused self-killing during sexual reproduction.

(E) Fusing an artificial PY motif (artPY) to Cw9ki abolished the toxicity of Cw9ki and converted Cw9ki to an antidote.

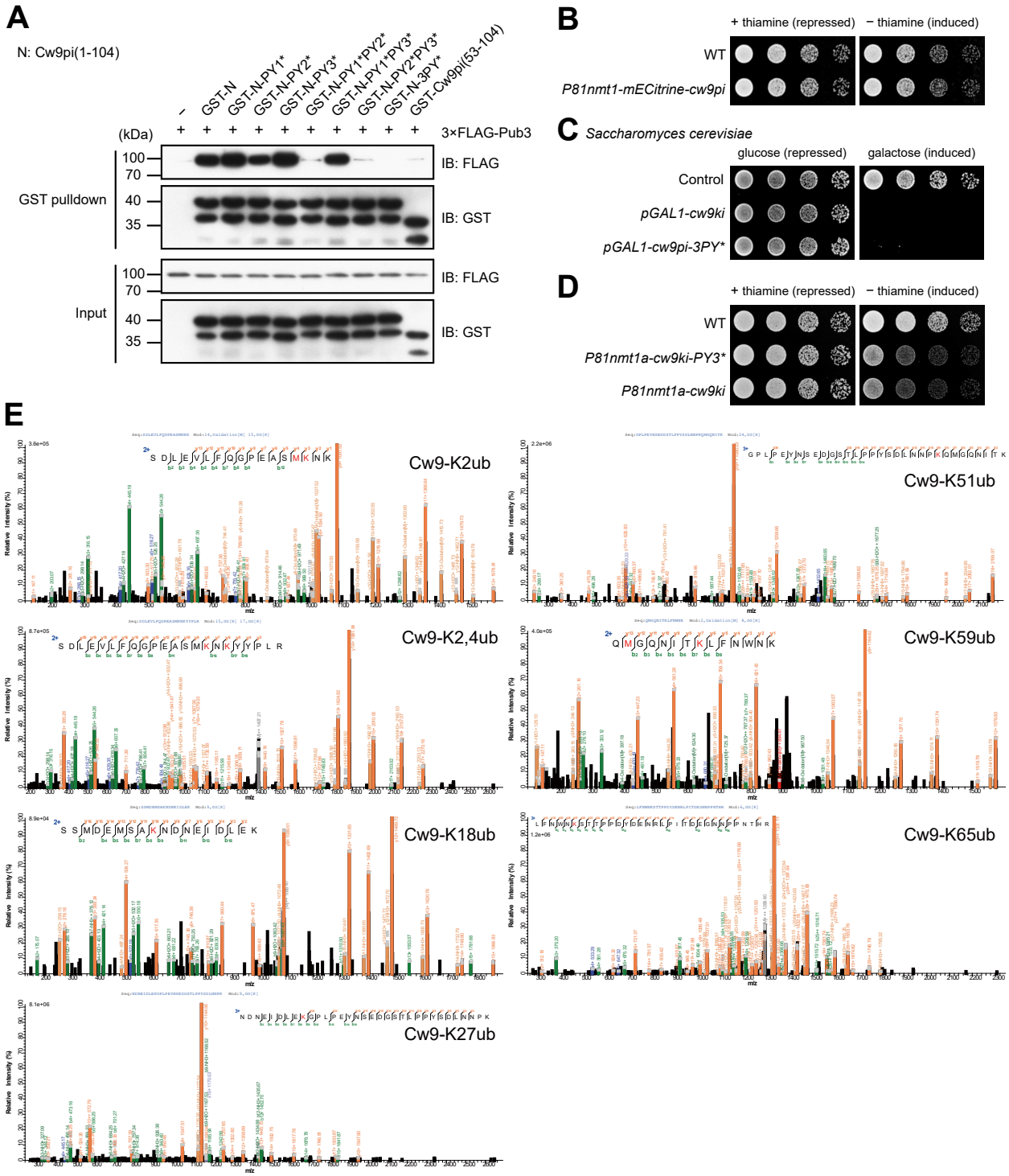

Figure S2. Related to Figure 3 and Figure 4.

(A) GST pulldown assay showed that PY motifs in the N-terminal cytosolic tail of Cw9pi mediate Pub3 binding. Lysates of *E. coli* cells expressing GST-tagged Cw9pi N-terminal

fragments were mixed with the lysate of *S. pombe* cells expressing 3xFLAG-Pub3 and pulldown was performed using glutathione beads.
(B) mECitrine-Cw9pi showed no toxicity to vegetative *S. pombe* cells.
(C) Cw9pi-3PY* was toxic to vegetative *S. cerevisiae* cells when expressed from the *pGAL1* promoter.
(D) Mutating PY3 in Cw9ki did not affect its toxicity. Expression was under the control of the *P81nmt1a* promoter, which is an attenuated version of the *P81nmt1* promoter.
(E) Representative mass spectrometry spectra of ubiquitinated peptides from in vitro ubiquitinated GST-Cw9pi(1-104).

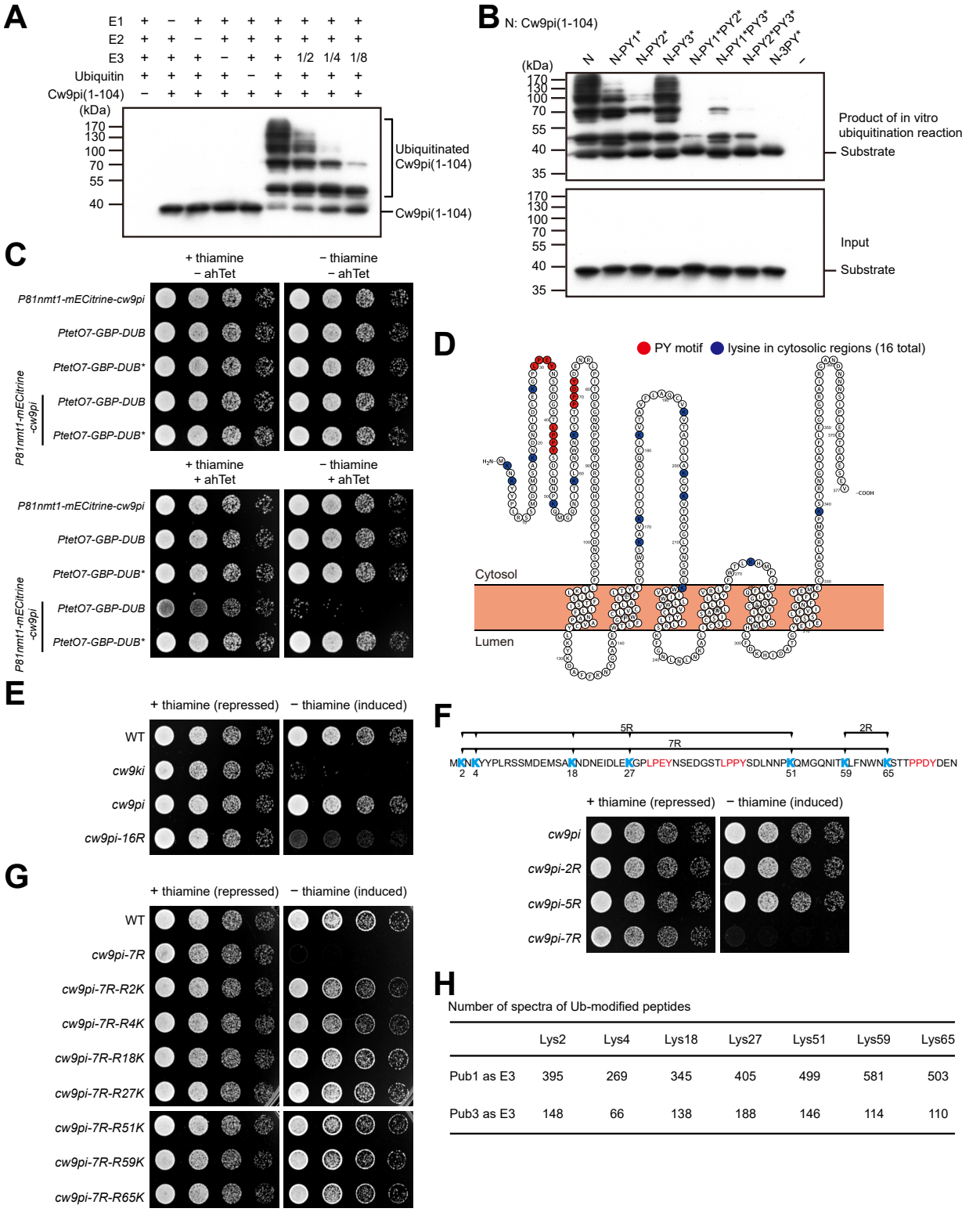

	Lys2	Lys4	Lys18	Lys27	Lys51	Lys59	Lys65
Pub1 as E3	395	269	345	405	499	581	503
Pub3 as E3	148	66	138	188	146	114	110

Figure 4. PY motif-dependent ubiquitination of the N-terminal cytosolic tail of Cw9pi renders Cw9pi non-toxic.

(A) Pub1-catalyzed in vitro ubiquitination of Cw9pi(1-104). All components of the in vitro ubiquitination reactions were purified from *E. coli*. Immunoblotting was used to detect Cw9pi(1-104), which was fused to a lysine-free 8×myc* tag that can be recognized by the myc antibody.[57]
(B) PY motif mutations diminished the in vitro ubiquitination of Cw9pi(1-104).
(C) Tethering a de-ubiquitinating enzyme (DUB) UL36 to Cw9pi through the mECitrine-GBP interaction rendered Cw9pi toxic. UL36-C40S (DUB*) is a catalytically inactive mutant of UL36.
(D) Diagram highlighting lysines in the cytosolic regions of Cw9pi. Blue circles denote the 16 lysines residing in the cytosolic tails or loops, including K216, which is predicted to localize at the cytosolic edge of a transmembrane helix. Red circles denote the PY motifs. This diagram was generated using Protter.[65]
(E) Mutating all 16 lysines in the cytosolic regions of Cw9pi to arginines (16R) rendered Cw9pi toxic to vegetative cells. Expression was under the control of the *P41nmt1* promoter.
(F) Mutating all 7 lysines in the N-terminal cytosolic tail of Cw9pi (7R) rendered Cw9pi toxic, whereas mutating two subsets of the 7 lysines (5R and 2R) did not cause toxicity. Expression was under the control of the *P41nmt1* promoter.
(G) The 7 lysines in the N-terminal cytosolic tail of Cw9pi are redundantly required for preventing the toxicity. Mutated residues in the 7R mutant were individually reverted to lysine. Expression was under the control of the *P41nmt1* promoter.
(H) All seven lysines in the N-terminal cytosolic tail of Cw9pi can be ubiquitinated in vitro by Pub1 and Pub3. In vitro ubiquitination of GST-Cw9pi(1-104) was performed using either Pub1 or Pub3 as E3 and ubiquitination sites were identified by mass spectrometry.

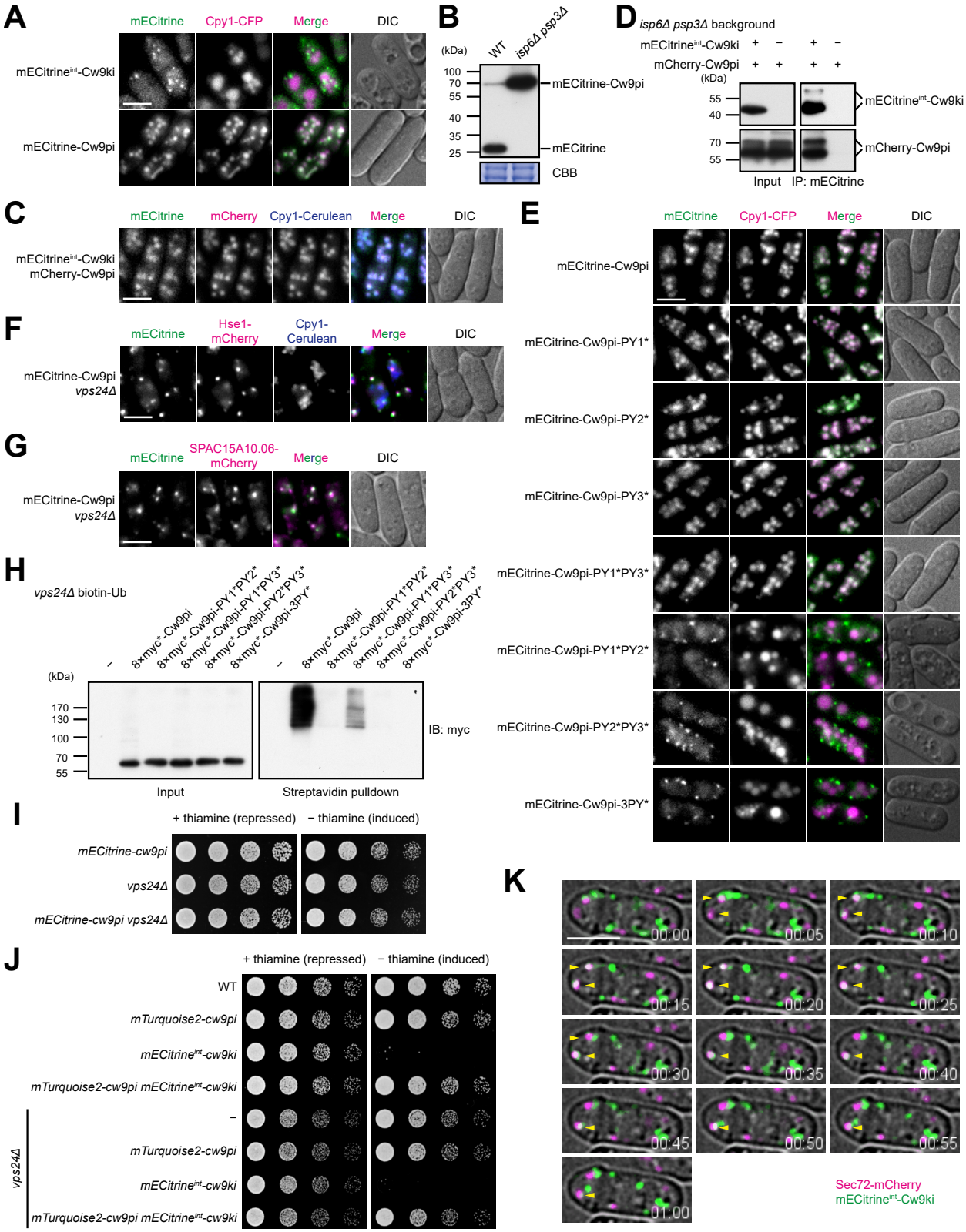

Figure 5. PY motif-dependent ubiquitination of Cw9pi promotes its trafficking from the

TGN to the endosome and from the endosome to the vacuole.
(A) Cw9ki localized to cytoplasmic puncta and Cw9pi localized to the vacuole lumen in vegetative *S. pombe* cells. Bar, 5 μm.
(B) mECitrine-Cw9pi was processed to free mECitrine in wild-type cells but not in cells lacking vacuolar proteases Isp6 and Psp3. Post-blotting staining of the PVDF membrane using Coomassie brilliant blue (CBB) served as the load control.
(C) Cw9ki exhibited a vacuole lumen localization when co-expressed with Cw9pi. Internally tagged Cw9ki was expressed from the *P81nmt1* promoter. N-terminally tagged Cw9pi was expressed from the *P41nmt1* promoter. Bar, 5 μm.
(D) Cw9pi coimmunoprecipitated with Cw9ki. Cw9ki was internally tagged and Cw9pi was N-terminally tagged. The *isp6Δ psp3Δ* background was used to ameliorate degradation.
(E) PY mutations that rendered Cw9pi toxic changed its localization to a Cw9ki-like cytoplasmic punctate pattern. Bar, 5 μm.
(F) Cw9pi co-localized with the endosome marker Hse1 in *vps24Δ* cells. Bar, 5 μm.
(G) Cw9pi co-localized with the endosome marker SPAC15A10.06 in *vps24Δ* cells. Bar, 5 μm.
(H) In vivo ubiquitination of Cw9pi in the *vps24Δ* background was diminished by PY mutations. Under a denaturing condition, biotin-tagged ubiquitin was precipitated using streptavidin beads and Cw9pi in the precipitates was detected by immunoblotting.
(I) Cw9pi remained non-toxic in *vps24Δ* cells. *vps24Δ* itself causes a slight growth defect. Cw9pi expression was under the control of the *P41nmt1* promoter.
(J) Cw9pi neutralized the toxicity of Cw9ki in the *vps24Δ* background. Cw9pi expression was under the control of the *P41nmt1* promoter and Cw9ki expression was under the control of the *P81nmt1* promoter.
(K) Time-lapse imaging showed that Cw9ki exhibited transient co-localization with the TGN marker Sec72. Yellow arrowheads indicate overlapping signals of Cw9ki and Sec72. Internally tagged Cw9ki was expressed from the *P81nmt1* promoter. Bar, 5 μm.

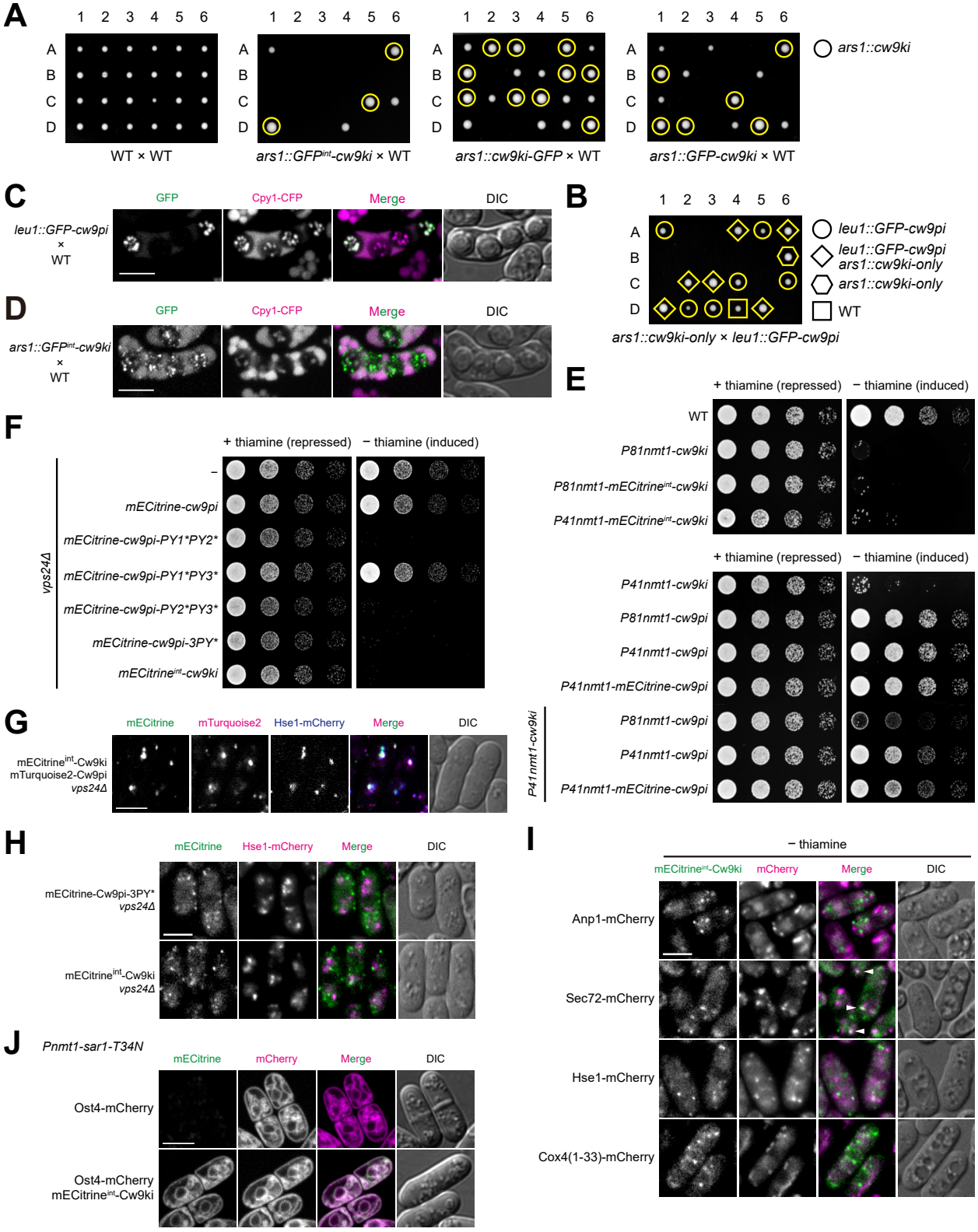

Figure S3. Related to Figure 5.

(A) When under the control of the native promoter, internally GFP-tagged Cw9ki exhibited a stronger spore killing than C-terminally and N-terminally tagged Cw9ki. A *ura4*$^{+}$ marker linked to the Cw9ki coding sequence caused faster growth of the surviving colonies containing the Cw9ki coding sequence.
(B) GFP-tagged Cw9pi under the control of the native promoter was able to neutralize the spore killing activity of Cw9ki.
(C) Cw9pi localized to the vacuole in spores. Cpy1-CFP is a vacuole lumen marker. Bar, 5 μm.
(D) Cw9ki localized to cytoplasmic puncta outside of vacuoles in spores. Bar, 5 μm.
(E) In vegetative cells, mECitrine-tagged Cw9ki caused growth inhibition and mECitrine-tagged Cw9pi conferred protection against Cw9ki.
(F) Cw9ki and the *PY1*PY2**, *PY2*PY3**, and *3PY** mutants of Cw9pi exhibited toxicity in the *vps24Δ* background. Expression was under the control of the *P81nmt1* promoter.
(G) Cw9ki localized to the endosome when co-expressed with Cw9pi in the *vps24Δ* background. Bar, 5 μm.
(H) Cw9pi-3PY* and Cw9ki did not co-localize with the endosome marker Hse1 in *vps24Δ* cells. Bar, 5 μm.
(I) Co-localization analysis of Cw9ki with markers of different subcellular organelles. Internally tagged Cw9ki was expressed from the *P81nmt1* promoter. Anp1-mCherry is a cis-Golgi marker. Sec72-mCherry is a TGN marker. Hse1-mCherry is an endosome marker. Cox4(1-33)-mCherry is a mitochondria marker. Arrowheads indicate overlapping signals of Cw9ki and Sec72. Bar, 5 μm.
(J) Overexpression of Sar1-T34N changed the localization of Cw9ki to the ER. Sar1-T34N was expressed from the *Pnmt1* promoter. Internally tagged Cw9ki was expressed from the *P81nmt1* promoter. Ost4-mCherry is an ER marker. Bar, 5 μm.

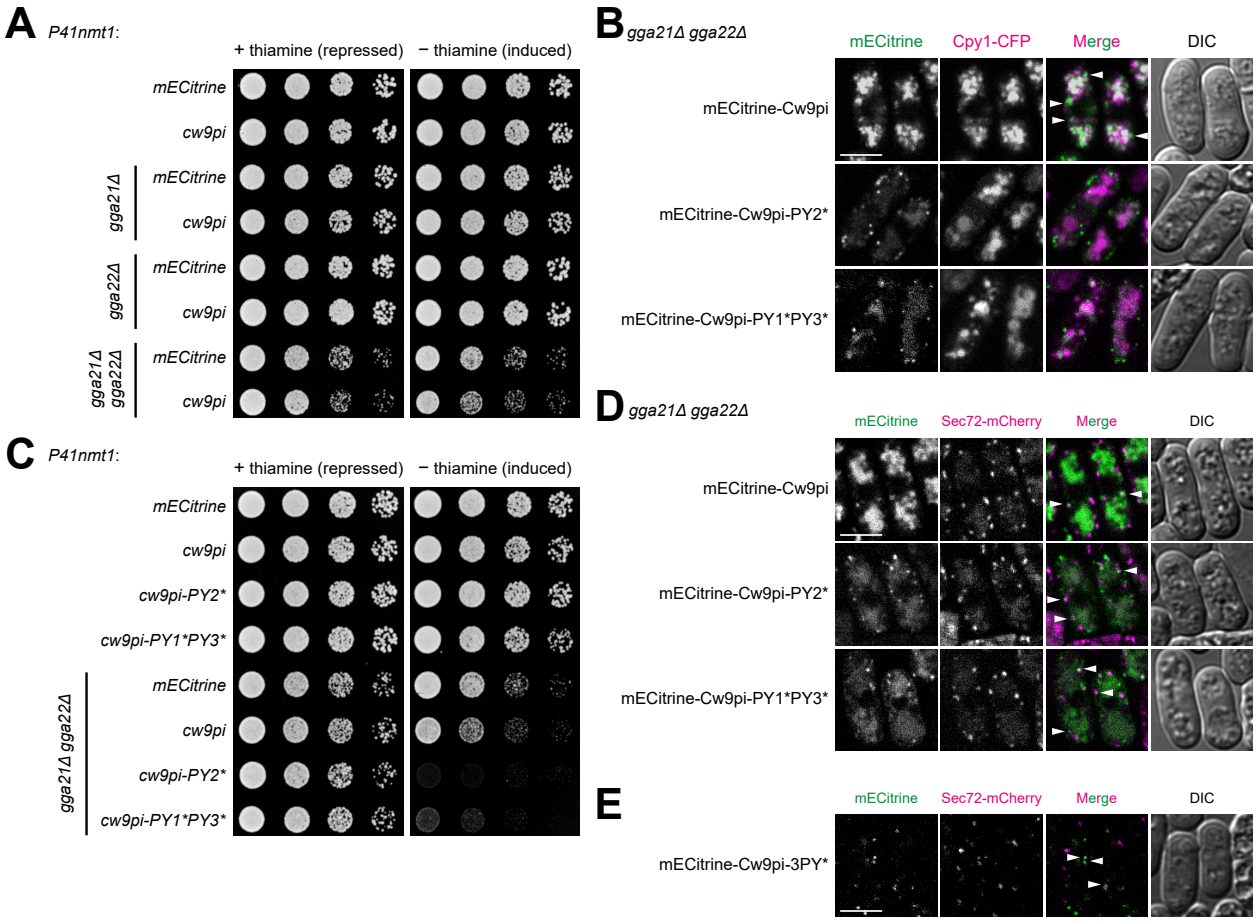

Figure S4. Related to Figure 5.

(A) Cw9pi caused a mild growth inhibition in the *gga21Δ gga22Δ* background.

(B) Localization of Cw9pi and its *PY2** and *PY1*PY3** mutants in the *gga21Δ gga22Δ* background. Expression was under the control of the *P41nmt1* promoter. Arrowheads indicate Cw9pi signals outside of vacuoles. Bar, 5 μm.

(C) The *PY2** and *PY1*PY3** mutants of Cw9pi exhibited strong toxicity in the *gga21Δ gga22Δ* background.

(D) Cytoplasmic puncta of Cw9pi and its *PY2** and *PY1*PY3** mutants partially co-localized with the TGN marker Sec72 in the *gga21Δ gga22Δ* background. Expression was under the control of the *P41nmt1* promoter. Arrowheads indicate signals overlapping with Sec72-mCherry. Bar, 5 μm.

(E) Cw9pi-3PY* partially co-localized with the TGN marker Sec72. N-terminally tagged Cw9pi-3PY* was expressed from the *P81nmt1* promoter. Arrowheads indicate signals overlapping with Sec72-mCherry. Bar, 5 μm.

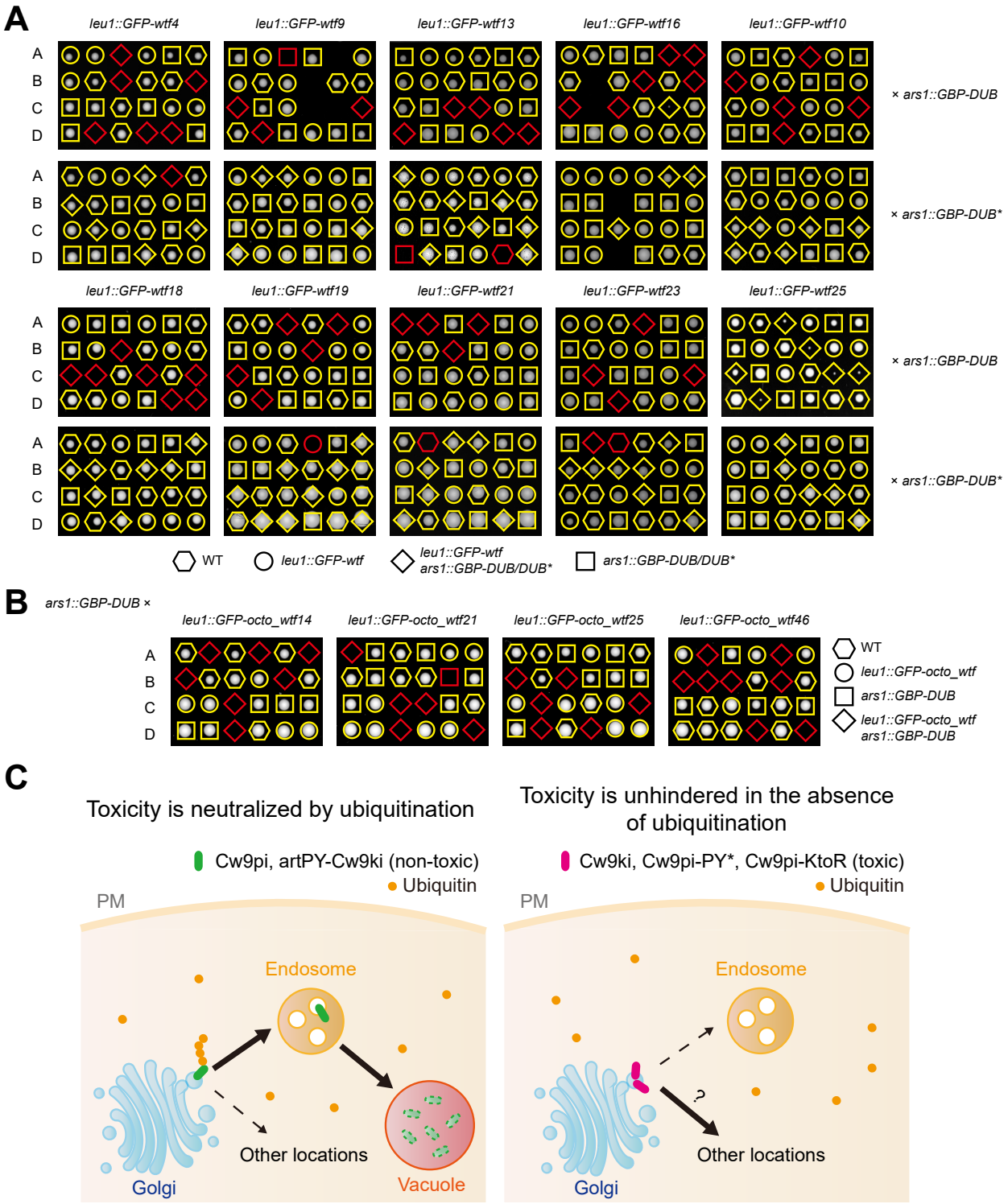

Figure 6. Antidote products of other *wtf* genes are kept non-toxic by ubiquitination.
(A) The antidote products of 10 *wtf* genes of the *S. pombe* reference genome were rendered toxic by artificial DUB tethering. Strains expressing a GFP-fused Wtf protein from the *P41nmt1* promoter were crossed to a strain expressing GBP-DUB or GBP-

DUB* from the *P41nmt1* promoter. Mating and sporulation were performed on thiamine-containing media and tetrad dissection was performed on thiamine-free media. Inviable spores whose genotype can be inferred assuming 2:2 segregation are indicated by red symbols.

(B) The antidote products of four *S. octosporus wtf* genes were rendered toxic by artificial DUB tethering. Experiments were performed as in A.

(C) A model of the role of PY motif-dependent ubiquitination in determining whether a Wtf protein is a poison or an antidote. PY motif-dependent ubiquitination diverts Wtf proteins from the TGN to the endosome, prevents toxicity, and confers antidote activities. Lack of ubiquitination results in the accumulation of Wtf proteins at the TGN and possibly other additional locations, and allows the manifestation of the toxicity.

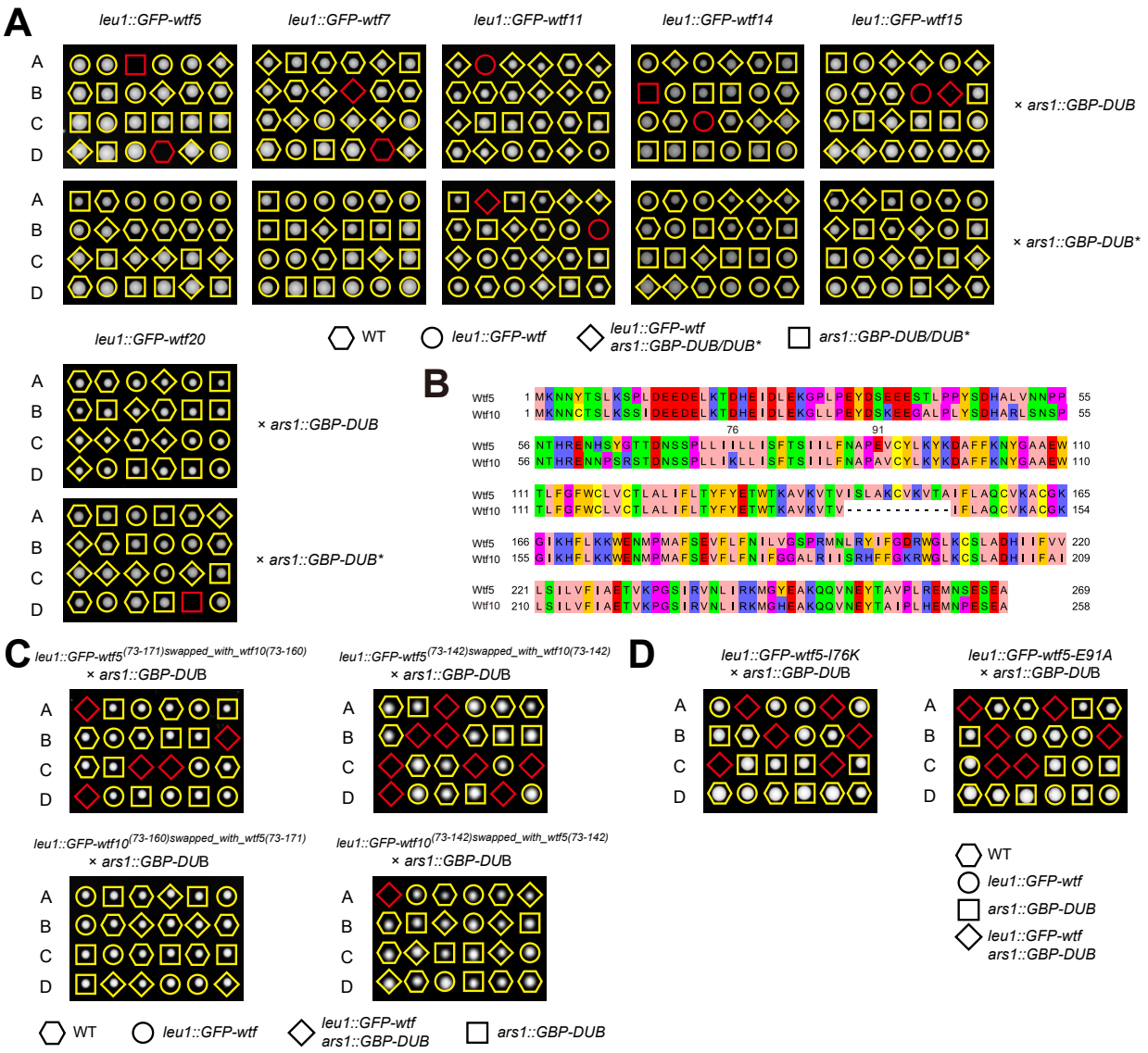

Figure S5. Related to Figure 6.

(A) The antidote products of six *S. pombe wtf* genes of the *S. pombe* reference genome were not rendered toxic by artificial DUB tethering. Experiments were performed as in Figure 6A.

(B) The sequence alignment of Wtf5 and Wtf10. The positions of the two residues (Ile76 and Glu91) affecting toxicity are shown.

(C) Sequence swapping between Wtf5 and Wtf10. Experiments were performed as in Figure 6A.

(D) Either an I76K mutation or an E91A mutation rendered Wtf5 toxic in the DUB tethering analysis. Experiments were performed as in Figure 6A.

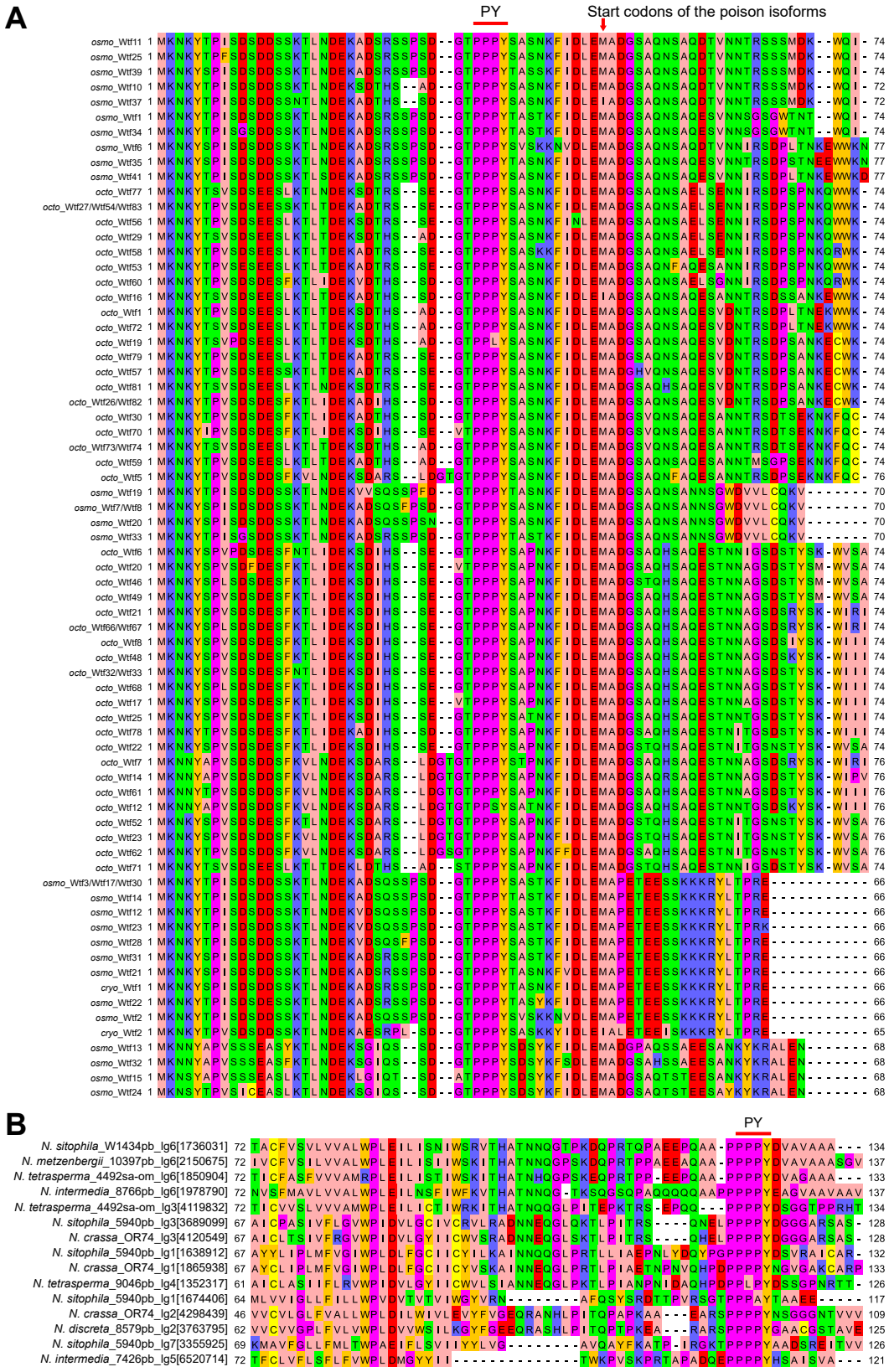

Figure S6. Related to Figure 6.

(A) Multiple sequence alignment of the N-terminal cytosolic tails of the antidote products encoded by *wtf* genes in *S. octosporus*, *S. osmophilus*, and *S. cryophilus*. Proteins sharing the same sequence in the N-terminal cytosolic tails are shown in a single row. The conserved PY motif is highlighted.
(B) Multiple sequence alignment of the C-terminal region of proteins encoded by representative *Spk-1* family genes. The conserved PY motif is highlighted.